Electronic Supplementary Material (ESI) for Digital Discovery.

Supplementary Information

Quantum circuit learning as a potential algorithm to predict experimental chemical properties

Kan Hatakeyama-Sato,* Yasuhiko Igarashi,
Takahiro Kashikawa, Koichi Kimura, Kenichi Oyaizu*

Table S1 Examples of simple quantum circuits and mathematical expressions.

NOTE: for simple expression, the results for $R_x(2t)$ and $R_y(2t)$ are used for $\hat{y}$ ($t \mapsto 2t$ in **Eq 4** and **Eq 5**).

Circuit	V	U	$\hat{y} = f_\theta(x)$
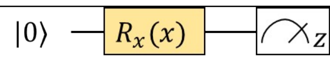	$R_x(x)$	-	$cos(2x)$
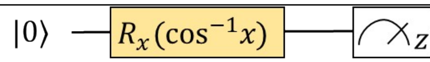	$R_x(\cos^{-1} x)$	-	$2x^2 - 1$
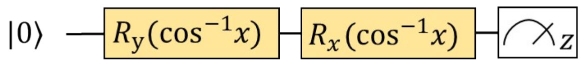	$R_x(\cos^{-1} x)$ $R_y(\cos^{-1} x)$	-	$4x^4 - 4x^2 - 1$
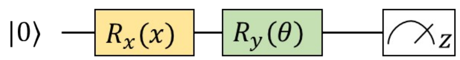	$R_x(x)$	$R_y(\theta)$	$\frac{\cos(2\theta - 2x)}{2} + \frac{\cos(2\theta + 2x)}{2}$
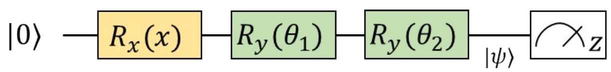	$R_x(x)$	$R_y(\theta_2)R_y(\theta_1)$	$-\frac{\cos(2\theta_2 - 2x)}{2} + \frac{\cos(2\theta_2 + 2x}{2}$ $+ \frac{\cos(-2\theta_1 + 2\theta_1 + 2x)}{4} + \frac{cos}{}$
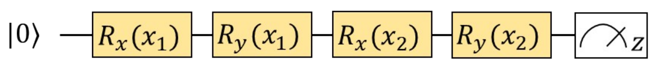	$R_y(x_2)R_x(x_2)$ $\cdot R_y(x_1)R_x(x_1)$	-	$\frac{\cos(4x_1)}{4} + \frac{\cos(4x_2)}{4} - \frac{\cos(2x_1}{4}$ $+ \frac{1}{4}$
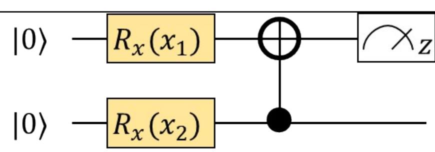	$R_x(x_1) \otimes R_x(x_2)$	$CNOT(2,1)$	$\frac{\cos(2x_1 - 2x_2)}{2} + \frac{\cos(2x_1 + 2x_2}{2}$

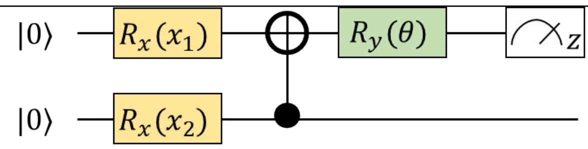	$R_x(x_1)\otimes R_x(x_2)$	$(R_y(\theta)\otimes I_2)\cdot CNO$	$\frac{\cos(-2\theta+2x_1+2x_2)}{4}+\frac{\cos(2}{}$
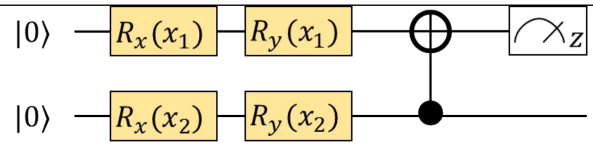	$(R_y(x_1)R_x(x_1))$ $\otimes(R_y(x_2)R_x(x_2)$ $)$	$CNOT(2,1)$	$(2\sin^2(x_1)-1)^2(2\sin^2(x_2)-1)^2$
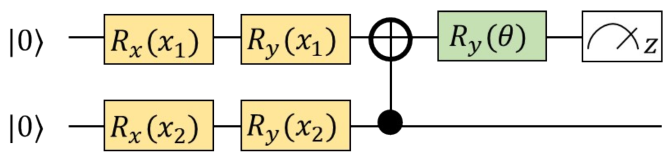	$(R_y(x_1)R_x(x_1))$ $\otimes(R_y(x_2)R_x(x_2)$ $)$	$(R_y(\theta)\otimes I_2)\cdot CNO$	$\frac{(1-\cos(2x_2))^2\cos(2\theta)}{2}+\frac{(1}{}$ $+\frac{\cos(2\theta-2x_2)}{2}+$ $+\frac{\cos(2\theta+4x_1+}{4}$
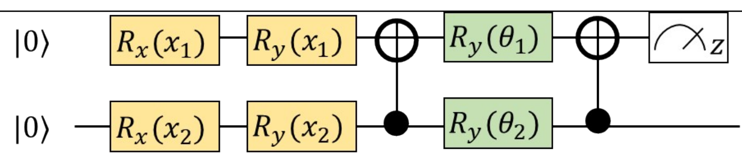	$(R_y(x_1)R_x(x_1))$ $\otimes(R_y(x_2)R_x(x_2)$ $)$	$CNOT(2,1)\cdot(R_y(\theta$	Eq S1
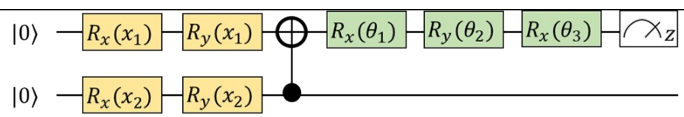	$(R_y(x_1)R_x(x_1))$ $\otimes(R_y(x_2)R_x(x_2)$ $)$	$\cdot(R_x(\theta_3)\otimes I_2)\cdot(R$	Eq S2
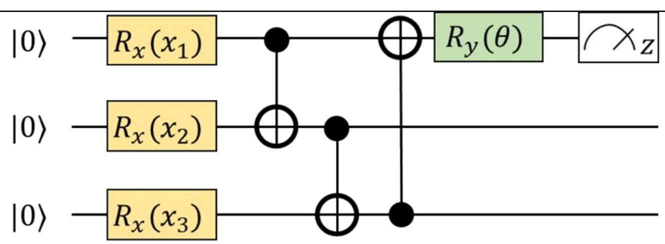	$R_x(x_1)$ $\otimes R_x(x_2)\otimes R_x(x_3)$	$(R_y(\theta)\otimes I_2\otimes I_2)$ $\cdot CNOT(3,1)$ $\cdot CNOT(2,3)$ $\cdot CNOT(1,2)$	Eq S3

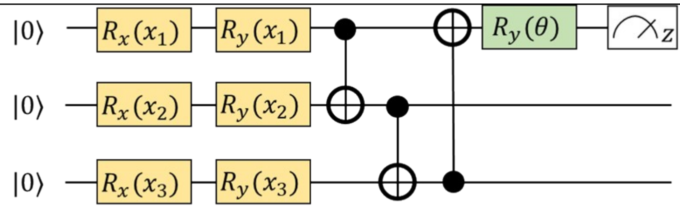	$(R_y(x_1)R_x(x_1)) \otimes (R_y(x_2)R_x(x_2)) \otimes (R_y(x_3)R_x(x_3))$	$(R_y(\theta)\otimes I_2\otimes I_2) \cdot CNOT(3,1) \cdot CNOT(2,3) \cdot CNOT(1,2)$	Eq S4

Eq S1

$$(1-\cos(2x_1))^2\cos(2\theta_2)-\frac{(1-\cos(2x_2))^2\cos(-2\theta_1+2\theta_2+4x_1)}{8}+\frac{(1-\cos(2x_2))^2\cos(2\theta_1-2\theta_2+4x_1)}{8}-\frac{(1-\cos(2x_2))^2\cos(2\theta_1+2\theta_2-4x_1)}{8}+\frac{(1-\cos(2x_2))^2\cos(2\theta_1+2\theta_2+4x_1)}{8}$$

$$+\frac{\sin(-2\theta_1+2\theta_2+4x_2)}{8}+\frac{\sin(2\theta_1-2\theta_2+4x_2)}{8}+\frac{\sin(2\theta_1+2\theta_2-4x_2)}{8}-\frac{\sin(2\theta_1+2\theta_2+4x_2)}{8}-\frac{\sin(-2\theta_1+2\theta_2+2x_1+2x_2)}{8}-\frac{\sin(2\theta_1-2\theta_2-2x_1+2x_2)}{8}-\frac{\sin(2\theta_1-2\theta_2+2x_1-2x_2)}{8}$$

$$+\frac{\sin(2\theta_1-2\theta_2+2x_1+2x_2)}{8}-\frac{\sin(2\theta_1+2\theta_2-2x_1-2x_2)}{8}+\frac{\sin(2\theta_1+2\theta_2-2x_1+2x_2)}{8}+\frac{\sin(2\theta_1+2\theta_2+2x_1-2x_2)}{8}-\frac{\sin(2\theta_1+2\theta_2+2x_1+2x_2)}{8}-\frac{3\cos(2\theta_2)}{2}+\frac{\cos(2\theta_1-2\theta_2)}{4}+\frac{\cos(2\theta_1+2\theta_2)}{4}$$

$$-\frac{\cos(2\theta_2-4x_1)}{4}+\cos(2\theta_2-2x_1)+\cos(2\theta_2+2x_1)-\frac{\cos(2\theta_2+4x_1)}{4}+\frac{\cos(-2\theta_1+2\theta_2+4x_1)}{4}+\frac{\cos(2\theta_1+2\theta_2-4x_1)}{4}-\frac{\cos(-2\theta_1+2\theta_2+4x_1+2x_2)}{8}-\frac{\cos(2\theta_1-2\theta_2-4x_1+2x_2)}{8}$$

$$+\frac{\cos(2\theta_1-2\theta_2+4x_1-2x_2)}{8}+\frac{\cos(2\theta_1-2\theta_2+4x_1+2x_2)}{8}-\frac{\cos(2\theta_1+2\theta_2-4x_1-2x_2)}{8}-\frac{\cos(2\theta_1+2\theta_2-4x_1+2x_2)}{8}+\frac{\cos(2\theta_1+2\theta_2+4x_1-2x_2)}{8}+\frac{\cos(2\theta_1+2\theta_2+4x_1+2x_2)}{8}$$

Eq S2

$$-\frac{(1-\cos(-2\theta_1+2\theta_2+2\theta_3))(\cos(4x_2)+1)}{32}-\frac{(1-\cos(2\theta_1-2\theta_2+2\theta_3))(\cos(4x_2)+1)}{32}-\frac{(1-\cos(2\theta_1+2\theta_2-2\theta_3))(\cos(4x_2)+1)}{32}-\frac{(1-\cos(2\theta_1+2\theta_2+2\theta_3))(\cos(4x_2)+1)}{32}$$

$$-\frac{(1-\cos(-2\theta_1+2\theta_2+2\theta_3+4x_1))(\cos(4x_2)+1)}{64}-\frac{(1-\cos(2\theta_1-2\theta_2-2\theta_3+4x_1))(\cos(4x_2)+1)}{64}-\frac{(1-\cos(2\theta_1-2\theta_2+2\theta_3-4x_1))(\cos(4x_2)+1)}{64}-\frac{(1-\cos(2\theta_1-2\theta_2+2\theta_3+4x_1))(\cos(4x_2)+1)}{64}$$

$$-\frac{(1-\cos(2\theta_1+2\theta_2-2\theta_3-4x_1))(\cos(4x_2)+1)}{64}-\frac{(1-\cos(2\theta_1+2\theta_2-2\theta_3+4x_1))(\cos(4x_2)+1)}{64}-\frac{(1-\cos(2\theta_1+2\theta_2+2\theta_3-4x_1))(\cos(4x_2)+1)}{64}-\frac{(1-\cos(2\theta_1+2\theta_2+2\theta_3+4x_1))(\cos(4x_2)+1)}{64}$$

$$+\frac{\cos(4x_2)}{4}-\frac{\cos(2\theta_1-2\theta_3)}{8}+\frac{\cos(2\theta_1+2\theta_3)}{8}+\frac{\cos(-2\theta_1+2\theta_2+2\theta_3)}{32}+\frac{\cos(-2\theta_1+2\theta_3+2x_1)}{8}-\frac{\cos(-2\theta_1+2\theta_3+4x_1)}{16}-\frac{\cos(-2\theta_1+2\theta_3+4x_2)}{16}+\frac{\cos(2\theta_1-2\theta_2+2\theta_3)}{32}+\frac{\cos(2\theta_1+2\theta_2-2\theta_3)}{32}$$

$$+\frac{\cos(2\theta_1+2\theta_2+2\theta_3)}{32}-\frac{\cos(2\theta_1-2\theta_3+2x_1)}{8}-\frac{\cos(2\theta_1-2\theta_3+4x_1)}{16}-\frac{\cos(2\theta_1-2\theta_3+4x_2)}{16}+\frac{\cos(2\theta_1+2\theta_3-4x_1)}{16}-\frac{\cos(2\theta_1+2\theta_3-2x_1)}{8}+\frac{\cos(2\theta_1+2\theta_3+2x_1)}{8}+\frac{\cos(2\theta_1+2\theta_3+4x_1)}{16}$$

$$+\frac{\cos(2\theta_1+2\theta_3-4x_2)}{16}+\frac{\cos(2\theta_1+2\theta_3+4x_2)}{16}-\frac{\cos(-2\theta_2+2\theta_3+4x_1)}{8}+\frac{\cos(2\theta_2-2\theta_3+4x_1)}{8}-\frac{\cos(2\theta_2+2\theta_3-4x_1)}{8}+\frac{\cos(2\theta_2+2\theta_3+4x_1)}{8}-\frac{\cos(-2\theta_1+2\theta_2+2\theta_3+2x_1)}{16}$$

$$+\frac{\cos(-2\theta_1+2\theta_2+2\theta_3+4x_1)}{64}+\frac{\cos(-2\theta_1+2\theta_2+2\theta_3+4x_2)}{64}+\frac{\cos(-2\theta_1+2\theta_3+2x_1+4x_2)}{16}-\frac{\cos(-2\theta_1+2\theta_3+4x_1+4x_2)}{32}+\frac{\cos(2\theta_1-2\theta_2-2\theta_3+2x_1)}{16}+\frac{\cos(2\theta_1-2\theta_2-2\theta_3+4x_1)}{64}$$

$$+\frac{\cos(2\theta_1-2\theta_2-2\theta_3+4x_2)}{64}+\frac{\cos(2\theta_1-2\theta_2+2\theta_3-4x_1)}{64}-\frac{\cos(2\theta_1-2\theta_2+2\theta_3-2x_1)}{16}+\frac{\cos(2\theta_1-2\theta_2+2\theta_3+2x_1)}{16}+\frac{\cos(2\theta_1-2\theta_2+2\theta_3+4x_1)}{64}+\frac{\cos(2\theta_1-2\theta_2+2\theta_3-4x_2)}{64}$$

$$+\frac{\cos(2\theta_1-2\theta_2+2\theta_3+4x_2)}{64}+\frac{\cos(2\theta_1+2\theta_2-2\theta_3-4x_1)}{64}-\frac{\cos(2\theta_1+2\theta_2-2\theta_3-2x_1)}{16}+\frac{\cos(2\theta_1+2\theta_2-2\theta_3+2x_1)}{16}+\frac{\cos(2\theta_1+2\theta_2-2\theta_3+4x_1)}{64}+\frac{\cos(2\theta_1+2\theta_2-2\theta_3-4x_2)}{64}$$

$$+\frac{\cos(2\theta_1+2\theta_2-2\theta_3+4x_2)}{64}+\frac{\cos(2\theta_1+2\theta_2+2\theta_3-4x_1)}{64}-\frac{\cos(2\theta_1+2\theta_2+2\theta_3-2x_1)}{16}+\frac{\cos(2\theta_1+2\theta_2+2\theta_3+2x_1)}{16}+\frac{\cos(2\theta_1+2\theta_2+2\theta_3+4x_1)}{64}+\frac{\cos(2\theta_1+2\theta_2+2\theta_3-4x_2)}{64}$$

$$+\frac{\cos(2\theta_1+2\theta_2+2\theta_3+4x_2)}{64}-\frac{\cos(2\theta_1-2\theta_3-4x_1+4x_2)}{32}+\frac{\cos(2\theta_1-2\theta_3-2x_1+4x_2)}{16}-\frac{\cos(2\theta_1-2\theta_3+2x_1-4x_2)}{16}-\frac{\cos(2\theta_1-2\theta_3+2x_1+4x_2)}{16}-\frac{\cos(2\theta_1-2\theta_3+4x_1-4x_2)}{32}$$

$$-\frac{\cos(2\theta_1-2\theta_3+4x_1+4x_2)}{32}+\frac{\cos(2\theta_1+2\theta_3-4x_1-4x_2)}{32}+\frac{\cos(2\theta_1+2\theta_3-4x_1+4x_2)}{32}-\frac{\cos(2\theta_1+2\theta_3-2x_1-4x_2)}{16}-\frac{\cos(2\theta_1+2\theta_3-2x_1+4x_2)}{16}+\frac{\cos(2\theta_1+2\theta_3+2x_1-4x_2)}{16}$$

$$+\frac{\cos(2\theta_1+2\theta_3+2x_1+4x_2)}{16}+\frac{\cos(2\theta_1+2\theta_3+4x_1-4x_2)}{32}+\frac{\cos(2\theta_1+2\theta_3+4x_1+4x_2)}{32}-\frac{\cos(-2\theta_1-2\theta_2+2\theta_3+2x_1+4x_2)}{32}+\frac{\cos(-2\theta_1-2\theta_2+2\theta_3+4x_1+4x_2)}{128}-\frac{\cos(-2\theta_1+2\theta_2-2\theta_3+2x_1+4x_2)}{32}$$

$$+\frac{\cos(-2\theta_1+2\theta_2-2\theta_3+4x_1+4x_2)}{128}+\frac{\cos(-2\theta_1+2\theta_2+2\theta_3-4x_1+4x_2)}{128}+\frac{\cos(-2\theta_1+2\theta_2+2\theta_3-2x_1+4x_2)}{32}-\frac{\cos(-2\theta_1+2\theta_2+2\theta_3+2x_1-4x_2)}{32}-\frac{\cos(-2\theta_1+2\theta_2+2\theta_3+2x_1+4x_2)}{32}$$

$$+\frac{\cos(-2\theta_1+2\theta_2+2\theta_3+4x_1-4x_2)}{128}+\frac{\cos(-2\theta_1+2\theta_2+2\theta_3+4x_1+4x_2)}{128}+\frac{\cos(2\theta_1-2\theta_2-2\theta_3+2x_1+4x_2)}{32}+\frac{\cos(2\theta_1-2\theta_2-2\theta_3+4x_1+4x_2)}{128}+\frac{\cos(2\theta_1-2\theta_2+2\theta_3-4x_1+4x_2)}{128}$$

$$-\frac{\cos(2\theta_1-2\theta_2+2\theta_3-2x_1+4x_2)}{32}+\frac{\cos(2\theta_1-2\theta_2+2\theta_3+2x_1-4x_2)}{32}+\frac{\cos(2\theta_1-2\theta_2+2\theta_3+2x_1+4x_2)}{32}+\frac{\cos(2\theta_1-2\theta_2+2\theta_3+4x_1-4x_2)}{128}+\frac{\cos(2\theta_1-2\theta_2+2\theta_3+4x_1+4x_2)}{128}$$

$$+\frac{\cos(2\theta_1+2\theta_2-2\theta_3-4x_1+4x_2)}{128}-\frac{\cos(2\theta_1+2\theta_2-2\theta_3-2x_1+4x_2)}{32}+\frac{\cos(2\theta_1+2\theta_2-2\theta_3+2x_1-4x_2)}{32}+\frac{\cos(2\theta_1+2\theta_2-2\theta_3+2x_1+4x_2)}{32}+\frac{\cos(2\theta_1+2\theta_2-2\theta_3+4x_1-4x_2)}{128}$$

$$+\frac{\cos(2\theta_1+2\theta_2-2\theta_3+4x_1+4x_2)}{128}+\frac{\cos(2\theta_1+2\theta_2+2\theta_3-4x_1-4x_2)}{128}+\frac{\cos(2\theta_1+2\theta_2+2\theta_3-4x_1+4x_2)}{128}-\frac{\cos(2\theta_1+2\theta_2+2\theta_3-2x_1-4x_2)}{32}-\frac{\cos(2\theta_1+2\theta_2+2\theta_3-2x_1+4x_2)}{32}$$

$$+\frac{\cos(2\theta_1+2\theta_2+2\theta_3+2x_1-4x_2)}{32}+\frac{\cos(2\theta_1+2\theta_2+2\theta_3+2x_1+4x_2)}{32}+\frac{\cos(2\theta_1+2\theta_2+2\theta_3+4x_1-4x_2)}{128}+\frac{\cos(2\theta_1+2\theta_2+2\theta_3+4x_1+4x_2)}{128}+\frac{1}{4}$$

Eq S3

$$2\left(\sin(\theta_{11y})\sin(x_1)\sin(x_2)+\cos(\theta_{11y})\cos(x_1)\cos(x_2)\right)^2\cos^2(x_3)+2\left(\sin(\theta_{11y})\sin(x_1)\cos(x_2)-\sin(x_2)\cos(\theta_{11y})\cos(x_1)\right)^2\sin^2(x_3)-1$$

Eq S4

$$-4\sin^2(\theta_{11y})\sin^4(x_1)+4\sin^2(\theta_{11y})\sin^2(x_1)-16\sin^2(\theta_{11y})\sin^4(x_2)\sin^4(x_3)+16\sin^2(\theta_{11y})\sin^4(x_2)\sin^2(x_3)-4\sin^2(\theta_{11y})\sin^4(x_2)+16\sin^2(\theta_{11y})\sin^2(x_2)\sin^4(x_3)-16\sin^2(\theta_{11y})\sin^2(x_2)\sin^2(x_3)+4\sin^2(\theta_{11y})\sin^2(x_2)-4\sin^2(\theta_{11y})\sin^4(x_3)+4\sin^2(\theta_{11y})\sin^2(x_3)-2\sin^2(\theta_{11y})-16\sin(\theta_{11y})\sin^3(x_1)\sin^3(x_2)\cos(\theta_{11y})\cos(x_1)\cos(x_2)+8\sin(\theta_{11y})\sin^3(x_1)\sin(x_2)\cos(\theta_{11y})\cos(x_1)\cos(x_2)+8\sin(\theta_{11y})\sin(x_1)\sin^3(x_2)\cos(\theta_{11y})\cos(x_1)\cos(x_2)+16\sin(\theta_{11y})\sin(x_1)\sin(x_2)\sin^4(x_3)\cos(\theta_{11y})\cos(x_1)\cos(x_2)-16\sin(\theta_{11y})\sin(x_1)\sin(x_2)\sin^2(x_3)\cos(\theta_{11y})\cos(x_1)\cos(x_2)+32\sin^4(x_1)\sin^4(x_2)\sin^4(x_3)-32\sin^4(x_1)\sin^4(x_2)\sin^2(x_3)+8\sin^4(x_1)\sin^4(x_2)-32\sin^4(x_1)\sin^2(x_2)\sin^4(x_3)+32\sin^4(x_1)\sin^2(x_2)\sin^2(x_3)-8\sin^4(x_1)\sin^2(x_2)+8\sin^4(x_1)\sin^4(x_3)-8\sin^4(x_1)\sin^2(x_3)+4\sin^4(x_1)-32\sin^2(x_1)\sin^4(x_2)\sin^4(x_3)+32\sin^2(x_1)\sin^4(x_2)\sin^2(x_3)-8\sin^2(x_1)\sin^4(x_2)+32\sin^2(x_1)\sin^2(x_2)\sin^4(x_3)-32\sin^2(x_1)\sin^2(x_2)\sin^2(x_3)+8\sin^2(x_1)\sin^2(x_2)-8\sin^2(x_1)\sin^4(x_3)+8\sin^2(x_1)\sin^2(x_3)-4\sin^2(x_1)+16\sin^4(x_2)\sin^4(x_3)-16\sin^4(x_2)\sin^2(x_3)+4\sin^4(x_2)-16\sin^2(x_2)\sin^4(x_3)+16\sin^2(x_2)\sin^2(x_3)-4\sin^2(x_2)+4\sin^4(x_3)-4\sin^2(x_3)+1$$

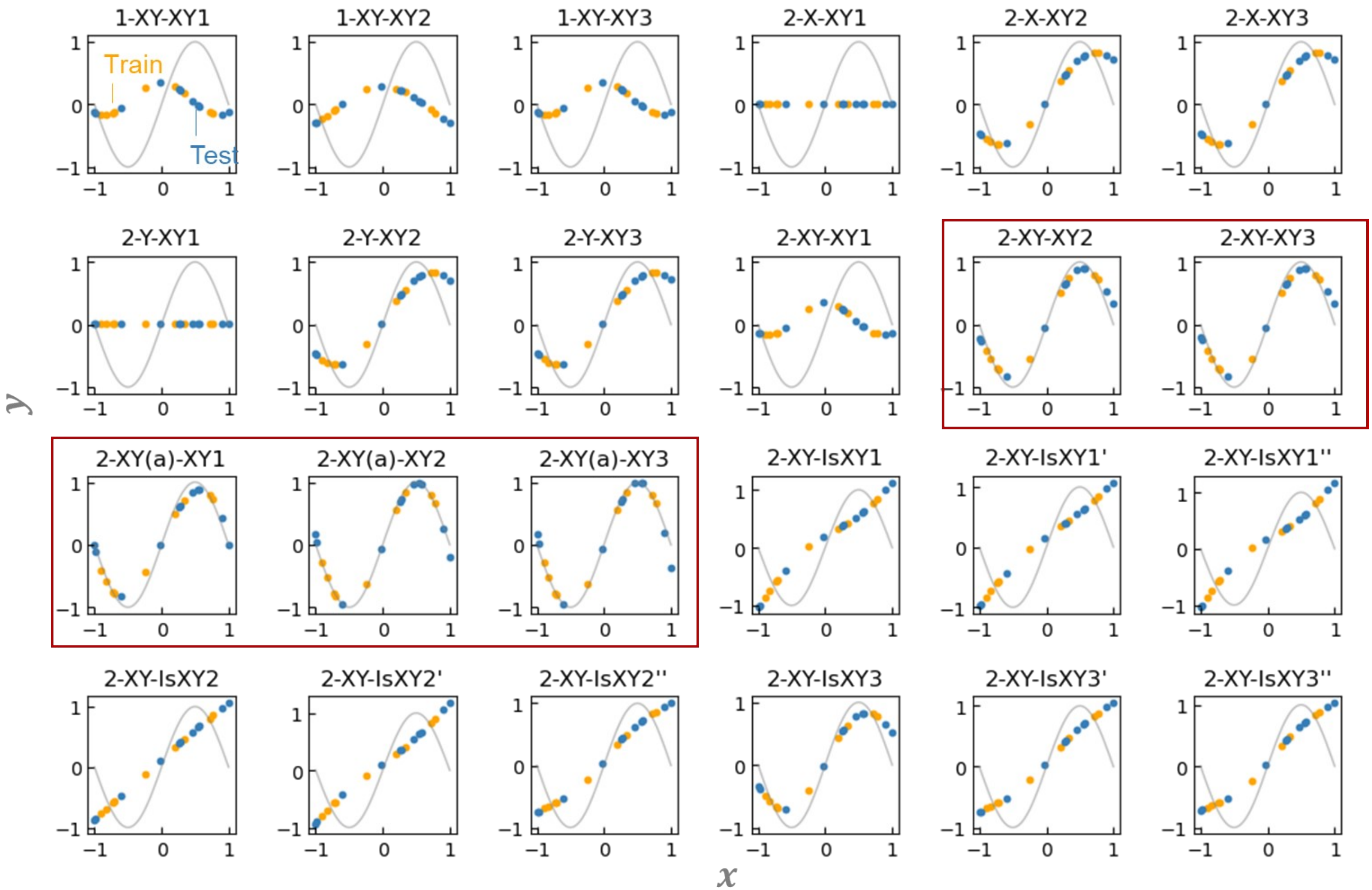
1-XY-XY1
Train
Test
1-XY-XY2
1-XY-XY3
2-X-XY1
2-X-XY2
2-X-XY3
2-Y-XY1
2-Y-XY2
2-Y-XY3
2-XY-XY1
2-XY-XY2
2-XY-XY3
2-XY(a)-XY1
2-XY(a)-XY2
2-XY(a)-XY3
2-XY-IsXY1
2-XY-IsXY1'
2-XY-IsXY1''
2-XY-IsXY2
2-XY-IsXY2'
2-XY-IsXY2''
2-XY-IsXY3
2-XY-IsXY3'
2-XY-IsXY3''
y
x

a)

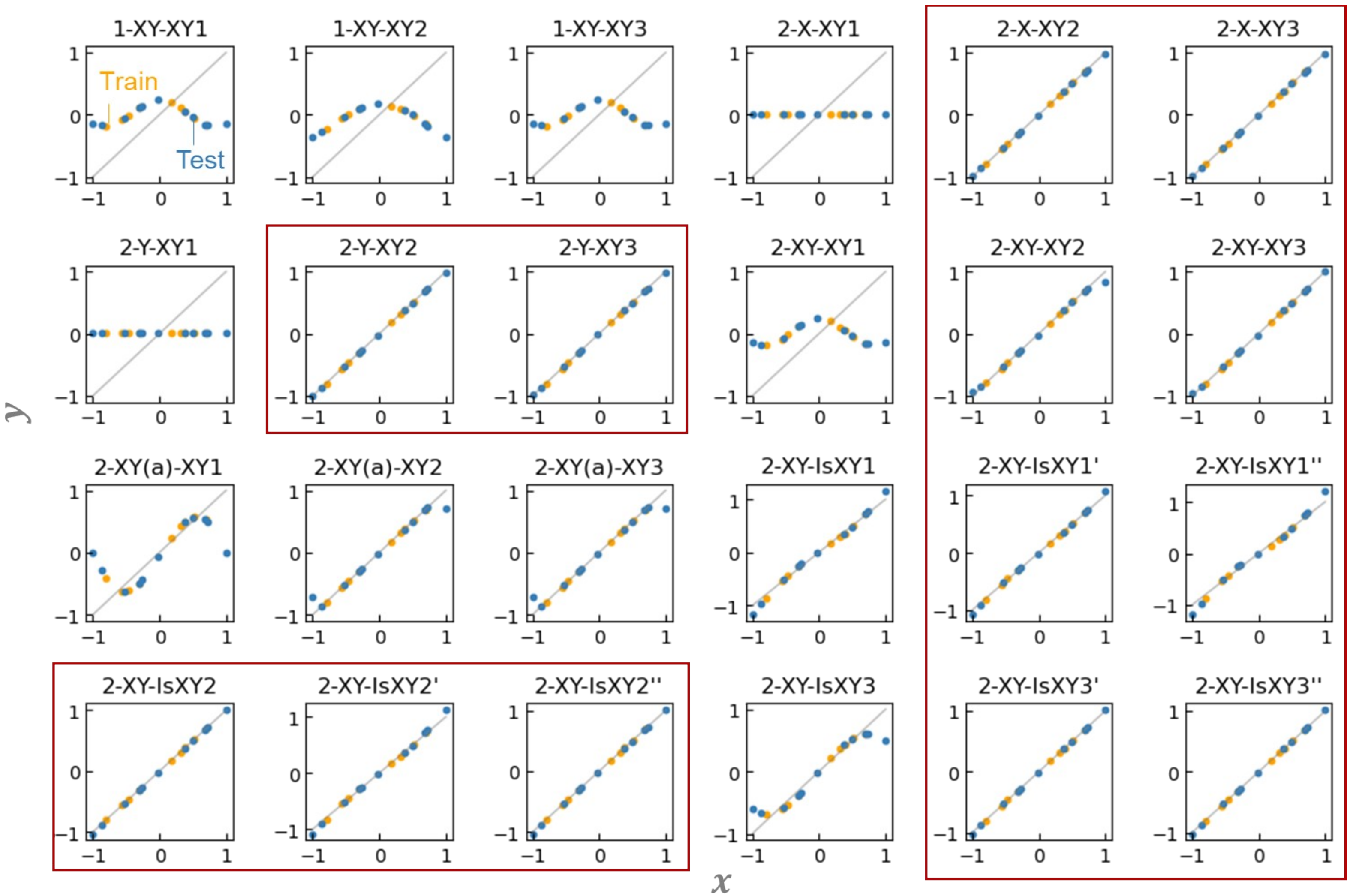

1-XY-XY1
1-XY-XY2
1-XY-XY3
2-X-XY1
2-X-XY2
2-X-XY3
2-Y-XY1
2-Y-XY2
2-Y-XY3
2-XY-XY1
2-XY-XY2
2-XY-XY3
2-XY(a)-XY1
2-XY(a)-XY2
2-XY(a)-XY3
2-XY-IsXY1
2-XY-IsXY1'
2-XY-IsXY1''
2-XY-IsXY2
2-XY-IsXY2'
2-XY-IsXY2''
2-XY-IsXY3
2-XY-IsXY3'
2-XY-IsXY3''
Train
Test
y
x

b)

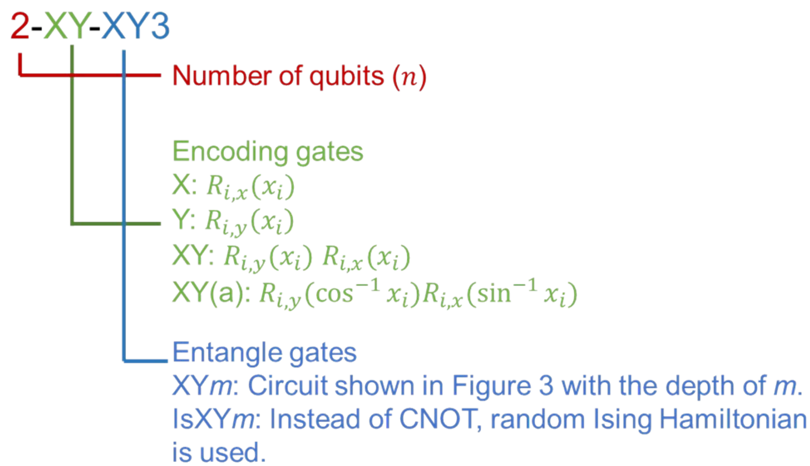

c)

Figure S 1 Regression results with different quantum circuits, fitting a) $y = \sin(x)$ and b) $y = x$. Successful results are marked red. Regressions were repeated three times with Ising-type circuits (IsXYm) because the results changed randomly. c) Explanation of circuit configuration.

NOTE: The best circuit configuration (2-XY-XYm) was selected for the following reasons. One qubit circuit could not fit the one-dimensional functions (e.g., 1-XY-XY3). For initial encoding, only the use of R_y gates was sufficient to fit the linear function (e.g., 2-Y-XY2 and 2-Y-XY3). However, additional R_x gates were needed for a non-linear $\sin(x)$ function (e.g., 2-XY-XY2 and 2-XY-XY3). Preprocessing of explanatory variables with $\cos^{-1} x_i$ and $\sin^{-1} x_i$ was not successful with the linear function (e.g., 2-XY(a)-XY3). The use of Ising Hamiltonian instead of CNOT circuits led to more unstable regressions due to the randomness (e.g., 2-XY-IsXY3).

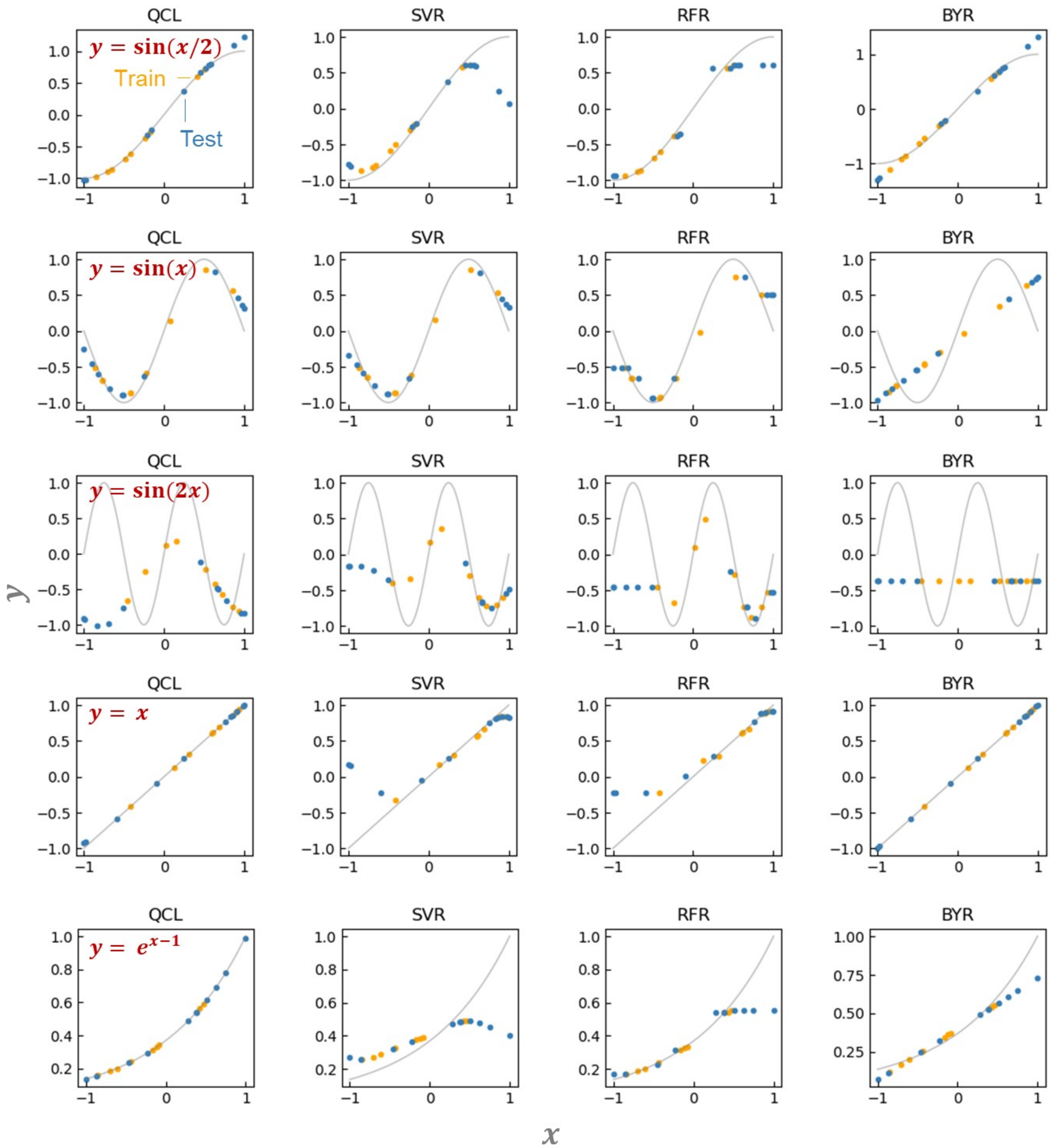

Figure S 2 Full regression results for Figure 4a.

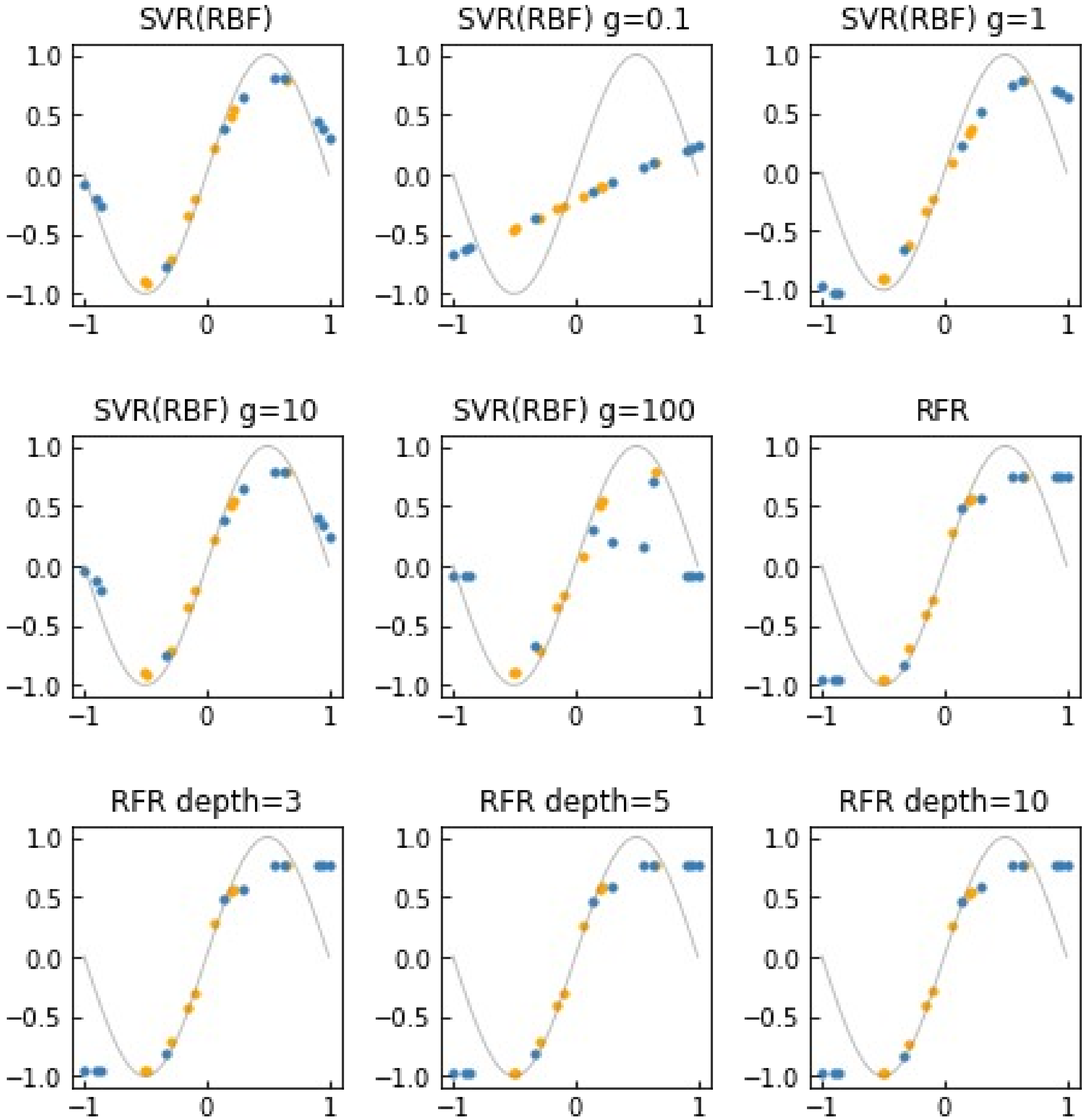
SVR(RBF)
SVR(RBF) g=0.1
SVR(RBF) g=1
SVR(RBF) g=10
SVR(RBF) g=100
RFR
RFR depth=3
RFR depth=5
RFR depth=10

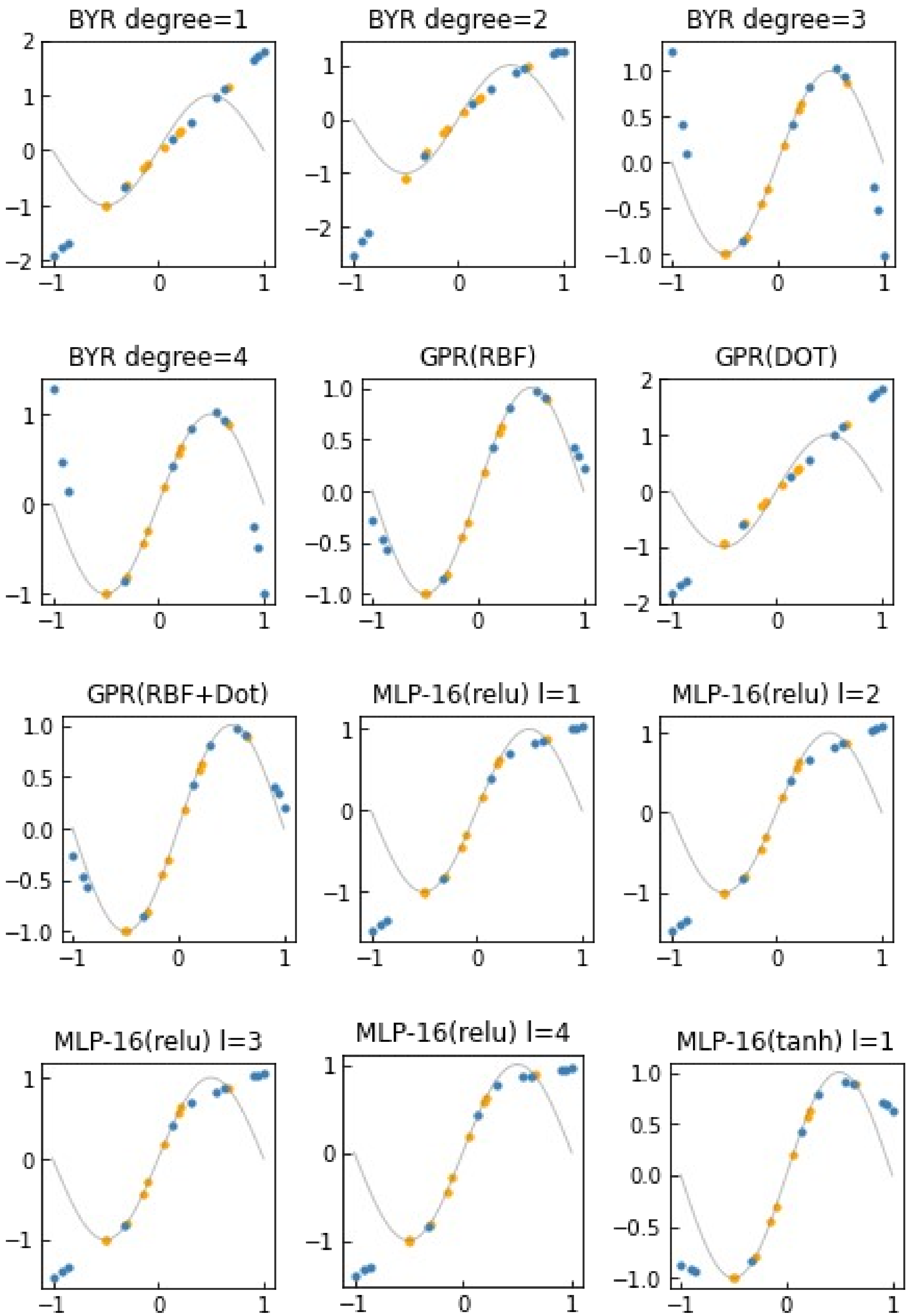
BYR degree=1
BYR degree=2
BYR degree=3
BYR degree=4
GPR(RBF)
GPR(DOT)
GPR(RBF+Dot)
MLP-16(relu) l=1
MLP-16(relu) l=2
MLP-16(relu) l=3
MLP-16(relu) l=4
MLP-16(tanh) l=1

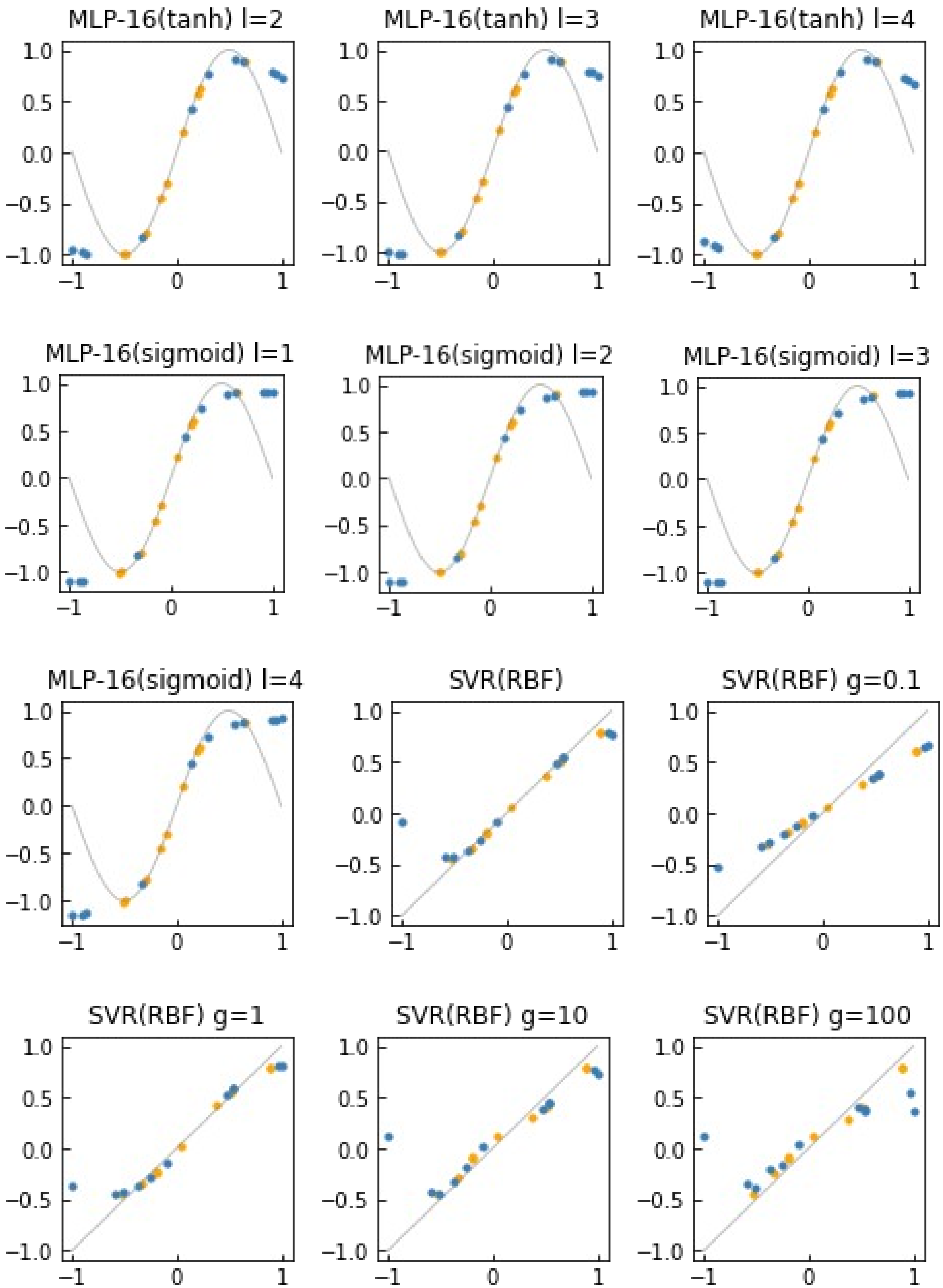
MLP-16(tanh) l=2
MLP-16(tanh) l=3
MLP-16(tanh) l=4
MLP-16(sigmoid) l=1
MLP-16(sigmoid) l=2
MLP-16(sigmoid) l=3
MLP-16(sigmoid) l=4
SVR(RBF)
SVR(RBF) g=0.1
SVR(RBF) g=1
SVR(RBF) g=10
SVR(RBF) g=100

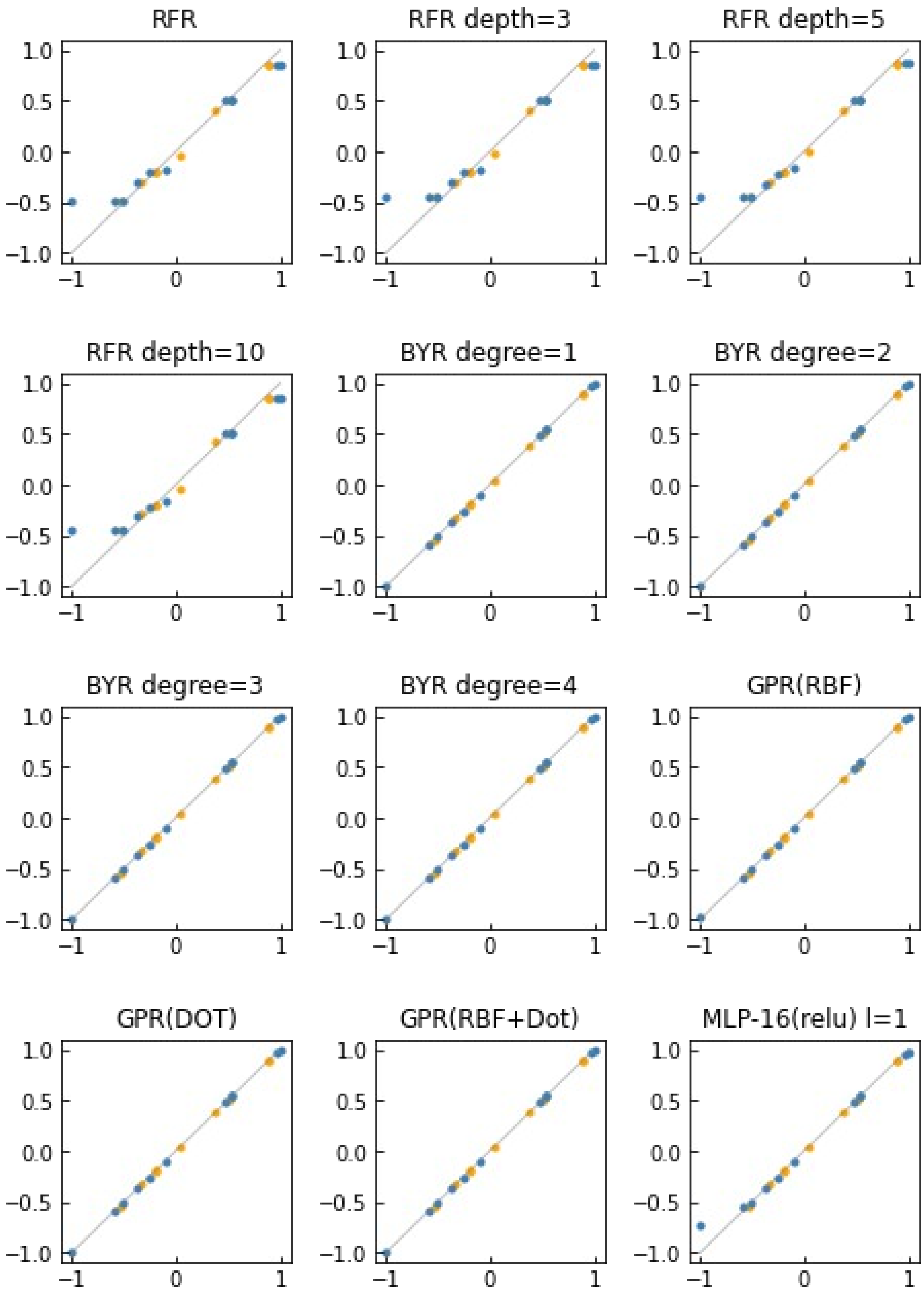
RFR
RFR depth=3
RFR depth=5
RFR depth=10
BYR degree=1
BYR degree=2
BYR degree=3
BYR degree=4
GPR(RBF)
GPR(DOT)
GPR(RBF+Dot)
MLP-16(relu) l=1
1.0
0.5
0.0
−0.5
−1.0
−1
0
1

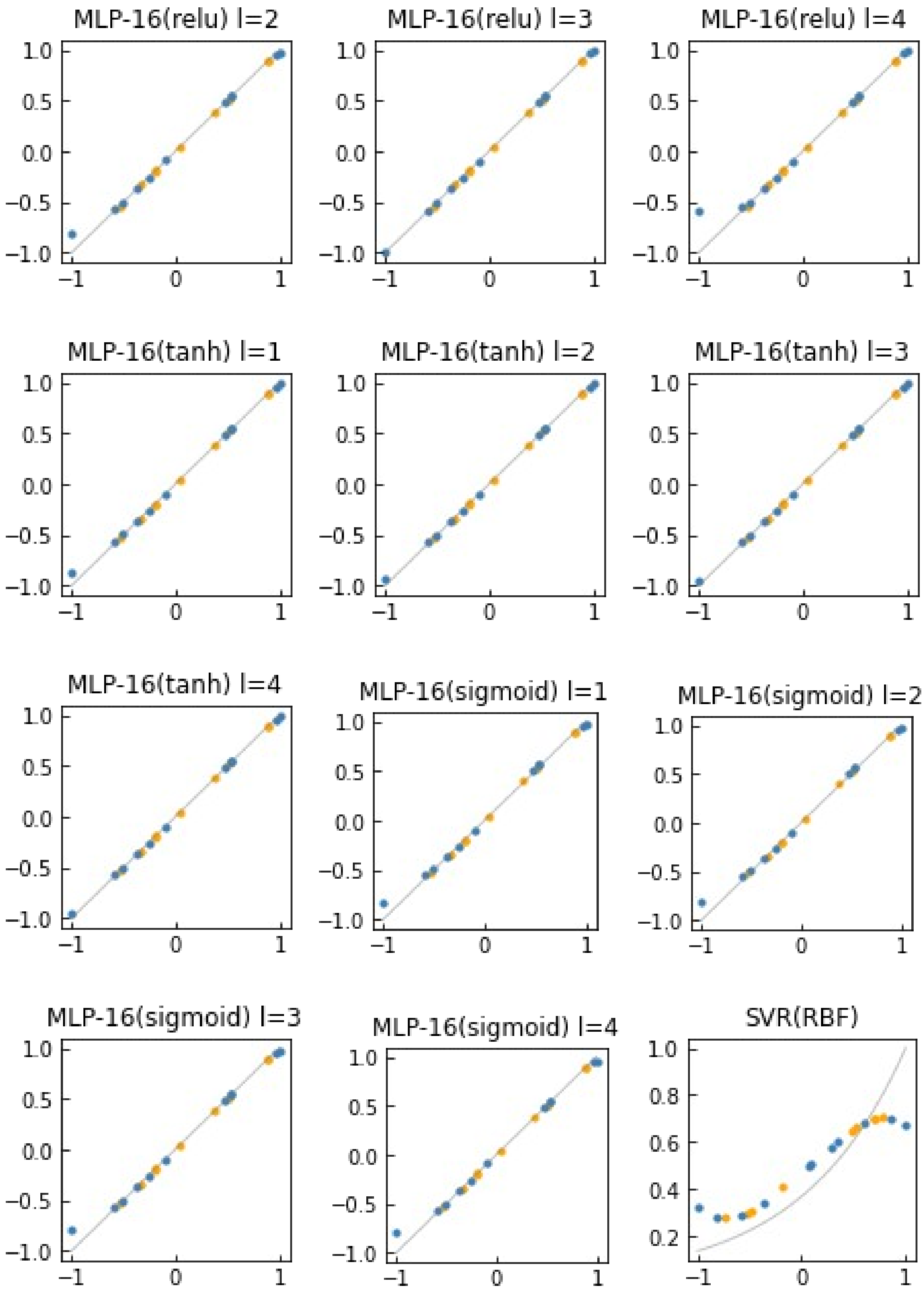

MLP-16(relu) l=2
MLP-16(relu) l=3
MLP-16(relu) l=4
MLP-16(tanh) l=1
MLP-16(tanh) l=2
MLP-16(tanh) l=3
MLP-16(tanh) l=4
MLP-16(sigmoid) l=1
MLP-16(sigmoid) l=2
MLP-16(sigmoid) l=3
MLP-16(sigmoid) l=4
SVR(RBF)
1.0
0.5
0.0
−0.5
−1.0
0.8
0.6
0.4
0.2
−1
0
1

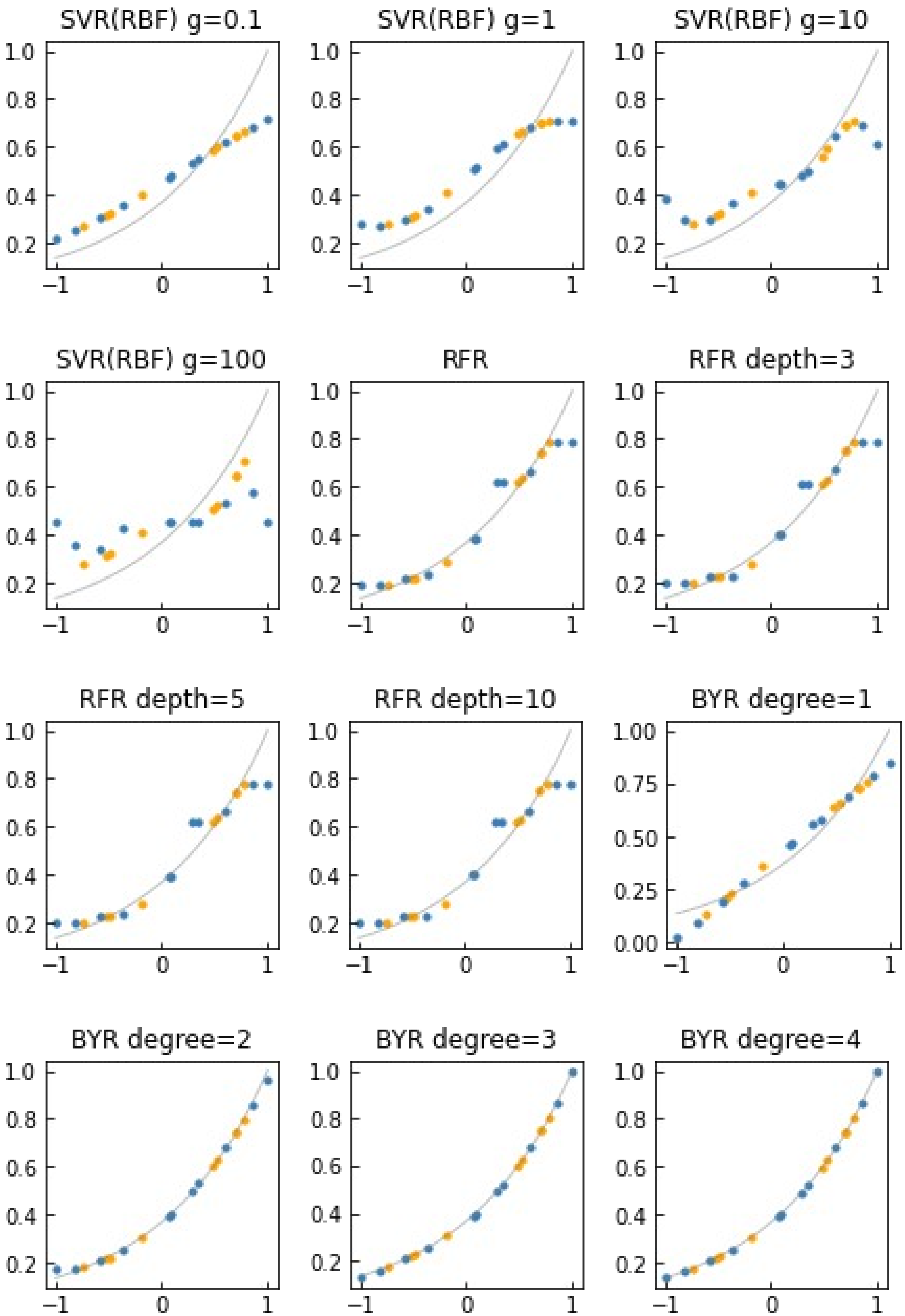

SVR(RBF) g=0.1
SVR(RBF) g=1
SVR(RBF) g=10
SVR(RBF) g=100
RFR
RFR depth=3
RFR depth=5
RFR depth=10
BYR degree=1
BYR degree=2
BYR degree=3
BYR degree=4

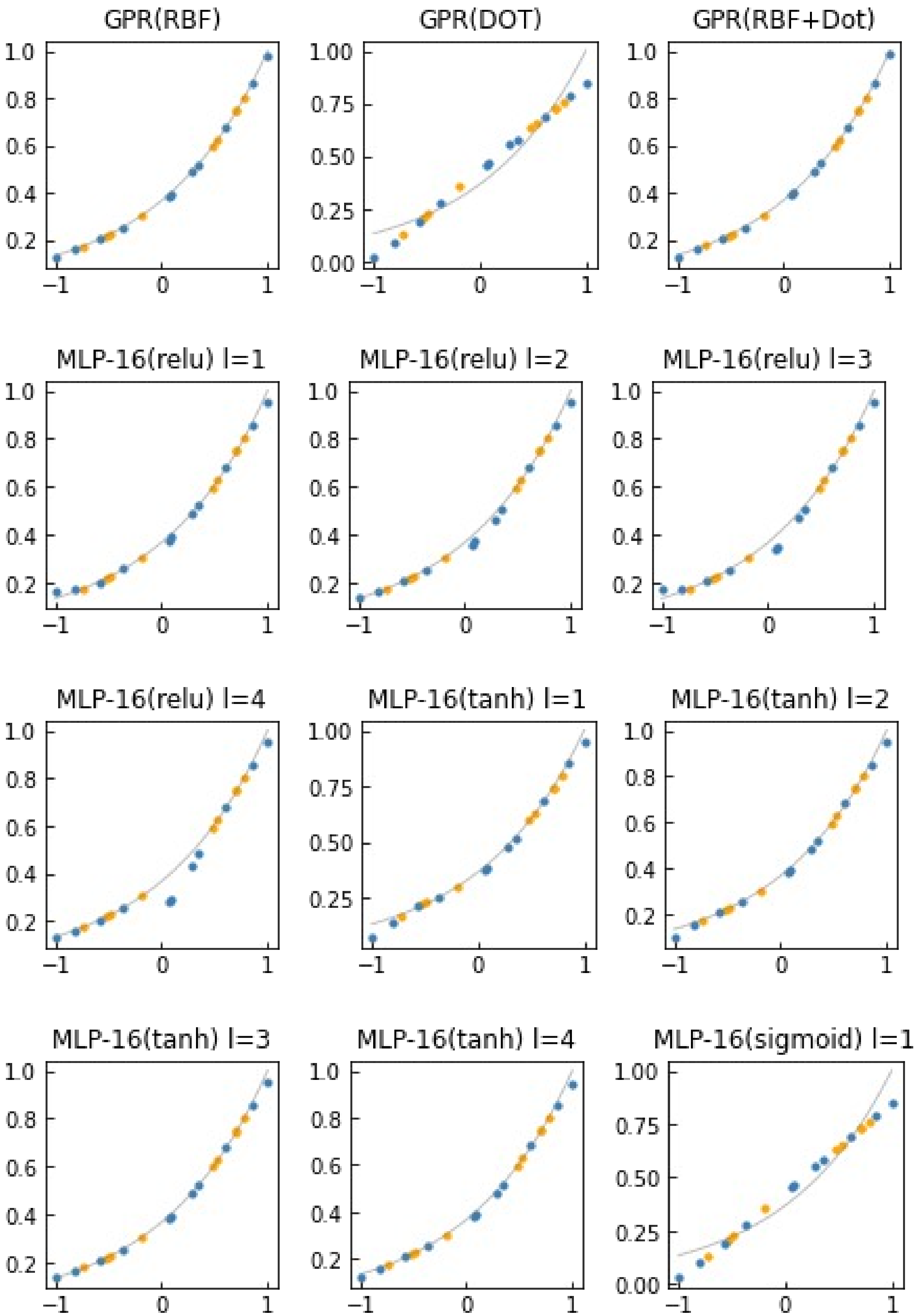
GPR(RBF)
GPR(DOT)
GPR(RBF+Dot)
MLP-16(relu) l=1
MLP-16(relu) l=2
MLP-16(relu) l=3
MLP-16(relu) l=4
MLP-16(tanh) l=1
MLP-16(tanh) l=2
MLP-16(tanh) l=3
MLP-16(tanh) l=4
MLP-16(sigmoid) l=1

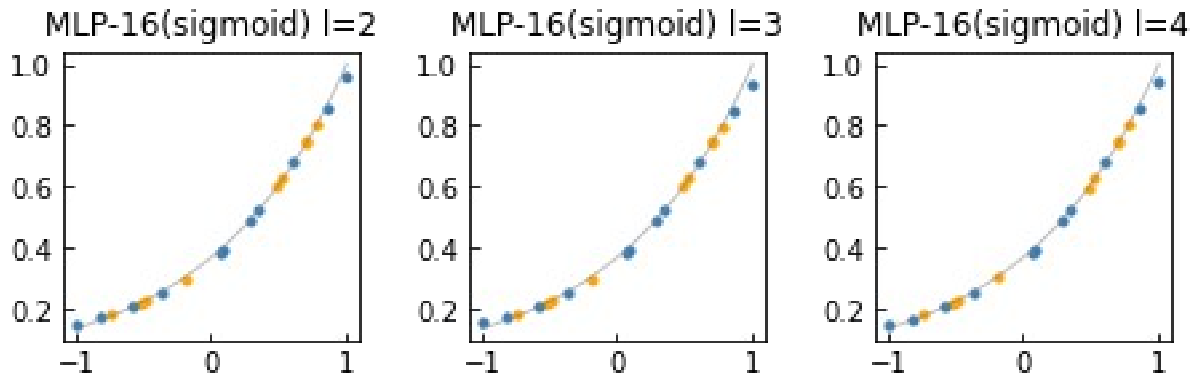

Figure S 3 Additional regression results for Figure S 2 using conventional machine learning models with various hyperparameters. Details of the models are explained in Table S2. The polynomial regression by BYR (degree > 1) could basically fit the three functions. However, the regression was unstable; it could easily induce overfitting and substantial prediction errors, as observed in Figure S 4 and Table S3.

Table S2 Explanations of the conventional models.[a)]

Expression	Model name	Hyperparameter
SVR(RBF)	SVR	kernel = “rbf”, gamma = “auto”
SVR(RBF) g=0.1	SVR	kernel = “rbf”, gamma = 0.1
SVR(RBF) g=1	SVR	kernel = “rbf” , gamma = 1
SVR(RBF) g=10	SVR	kernel = “rbf” , gamma = 10
SVR(RBF) g=100	SVR	kernel = “rbf” , gamma = 100
RFR	RandomForestRegressor	(default)
RFR depth=3	RandomForestRegressor	max_depth=3
RFR depth=5	RandomForestRegressor	max_depth=5
RFR depth=10	RandomForestRegressor	max_depth=10
BYR degree=1	BayesianRidge	(default)
BYR degree=2	BayesianRidge	(default) Convert x to $x + x^2$
BYR degree=3	BayesianRidge	(default) Convert x to $x + x^2 + x^3$
BYR degree=4	BayesianRidge	(default) Convert x to $x + x^2 ... + x^4$
GPR(RBF)	GaussianProcessRegressor	kernel=RBF + WhiteKernel
GPR(DOT)	GaussianProcessRegressor	kernel=DotProduct + WhiteKernel
GPR(RBF+Dot)	GaussianProcessRegressor	kernel=RBF+DotProduct + WhiteKernel
MLP-16(relu) l=1	Multi layer perceptron[b)]	One hidden layer, ReLu activation
MLP-16(relu) l=2	Multi layer perceptron[b)]	Two hidden layers, ReLu activation
MLP-16(relu) l=3	Multi layer perceptron[b)]	Three hidden layers, ReLu activation
MLP-16(relu) l=4	Multi layer perceptron[b)]	Four hidden layers, ReLu activation
MLP-16(tanh) l=1	Multi layer perceptron[b)]	One hidden layer, tanh activation
MLP-16(tanh) l=2	Multi layer perceptron[b)]	Two hidden layers, tanh activation
MLP-16(tanh) l=3	Multi layer perceptron[b)]	Three hidden layers, tanh activation
MLP-16(tanh) l=4	Multi layer perceptron[b)]	Four hidden layers, tanh activation
MLP-16(sigmoid) l=1	Multi layer perceptron[b)]	One hidden layer, sigmoid activation
MLP-16(sigmoid) l=2	Multi layer perceptron[b)]	Two hidden layers, sigmoid activation
MLP-16(sigmoid) l=3	Multi layer perceptron[b)]	Three hidden layers, sigmoid activation
MLP-16(sigmoid) l=4	Multi layer perceptron[b)]	Four hidden layers, sigmoid activation

a) Except for MLP, regressions models were made using a scikit-learn (version 1.0.2) library. Default hyperparameters were used unless noted otherwise. The document is available at https://scikit-learn.org/stable/whats_new/v1.0.html.
b) MLP was implemented by a Keras (version 2.9.0) library. The dimension of the hidden layers was 16.

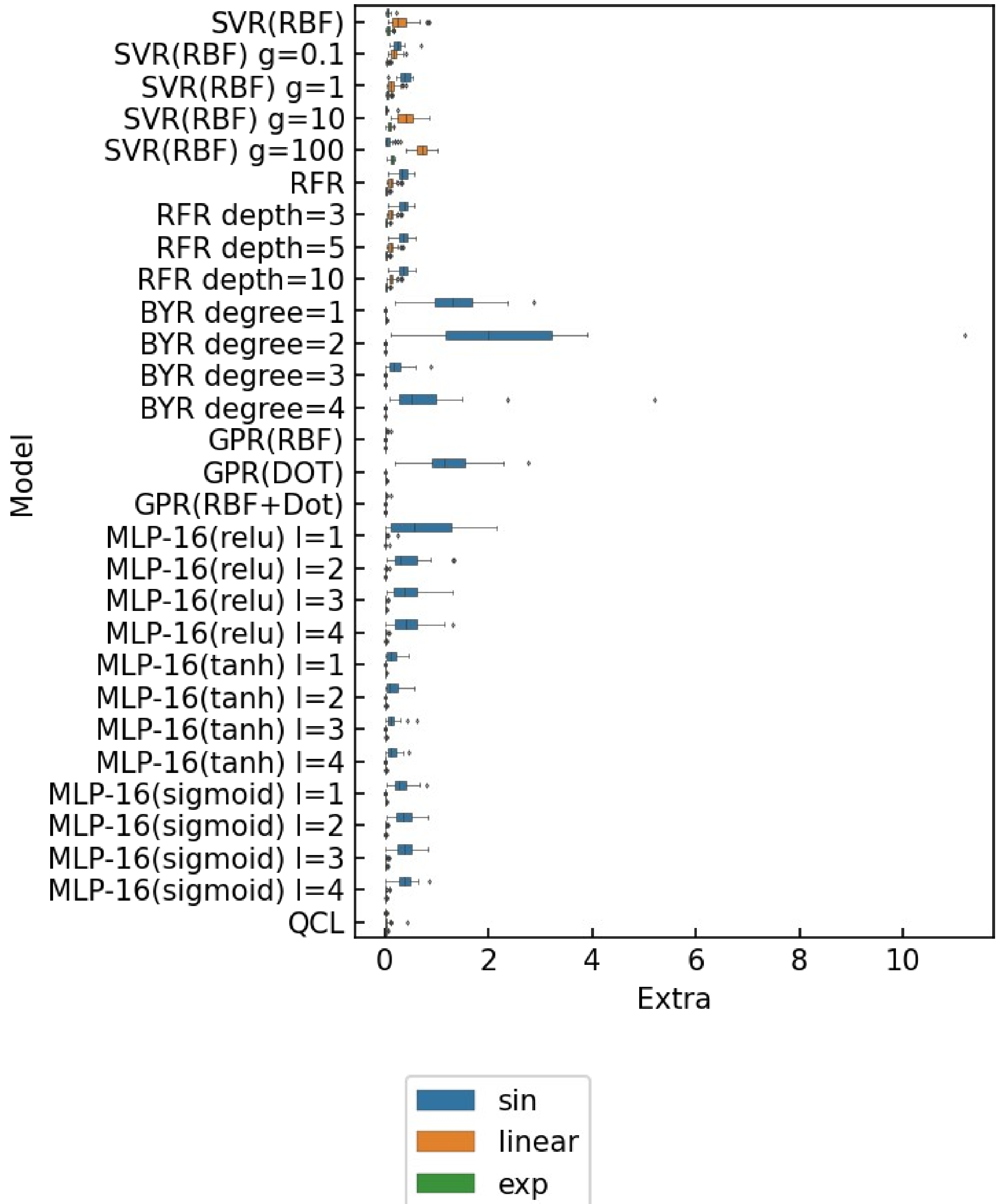

SVR(RBF)
SVR(RBF) g=0.1
SVR(RBF) g=1
SVR(RBF) g=10
SVR(RBF) g=100
RFR
RFR depth=3
RFR depth=5
RFR depth=10
BYR degree=1
BYR degree=2
BYR degree=3
BYR degree=4
GPR(RBF)
GPR(DOT)
GPR(RBF+Dot)
MLP-16(relu) l=1
MLP-16(relu) l=2
MLP-16(relu) l=3
MLP-16(relu) l=4
MLP-16(tanh) l=1
MLP-16(tanh) l=2
MLP-16(tanh) l=3
MLP-16(tanh) l=4
MLP-16(sigmoid) l=1
MLP-16(sigmoid) l=2
MLP-16(sigmoid) l=3
MLP-16(sigmoid) l=4
QCL
Model
0
2
4
6
8
10
Extra
sin
linear
exp

a)

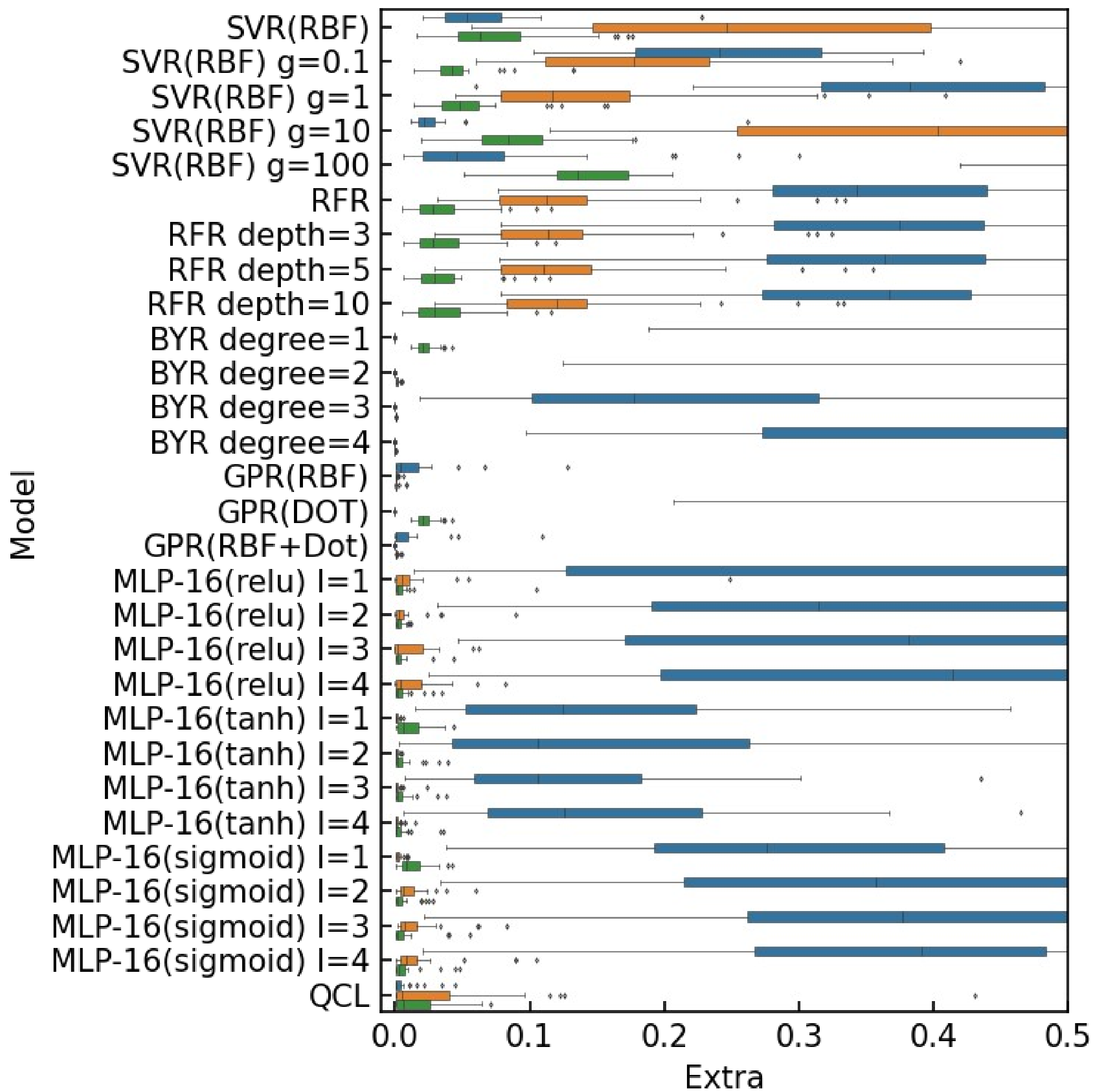
SVR(RBF)
SVR(RBF) g=0.1
SVR(RBF) g=1
SVR(RBF) g=10
SVR(RBF) g=100
RFR
RFR depth=3
RFR depth=5
RFR depth=10
BYR degree=1
BYR degree=2
BYR degree=3
BYR degree=4
GPR(RBF)
GPR(DOT)
GPR(RBF+Dot)
MLP-16(relu) l=1
MLP-16(relu) l=2
MLP-16(relu) l=3
MLP-16(relu) l=4
MLP-16(tanh) l=1
MLP-16(tanh) l=2
MLP-16(tanh) l=3
MLP-16(tanh) l=4
MLP-16(sigmoid) l=1
MLP-16(sigmoid) l=2
MLP-16(sigmoid) l=3
MLP-16(sigmoid) l=4
QCL
Model
0.0
0.1
0.2
0.3
0.4
0.5
Extra

b)

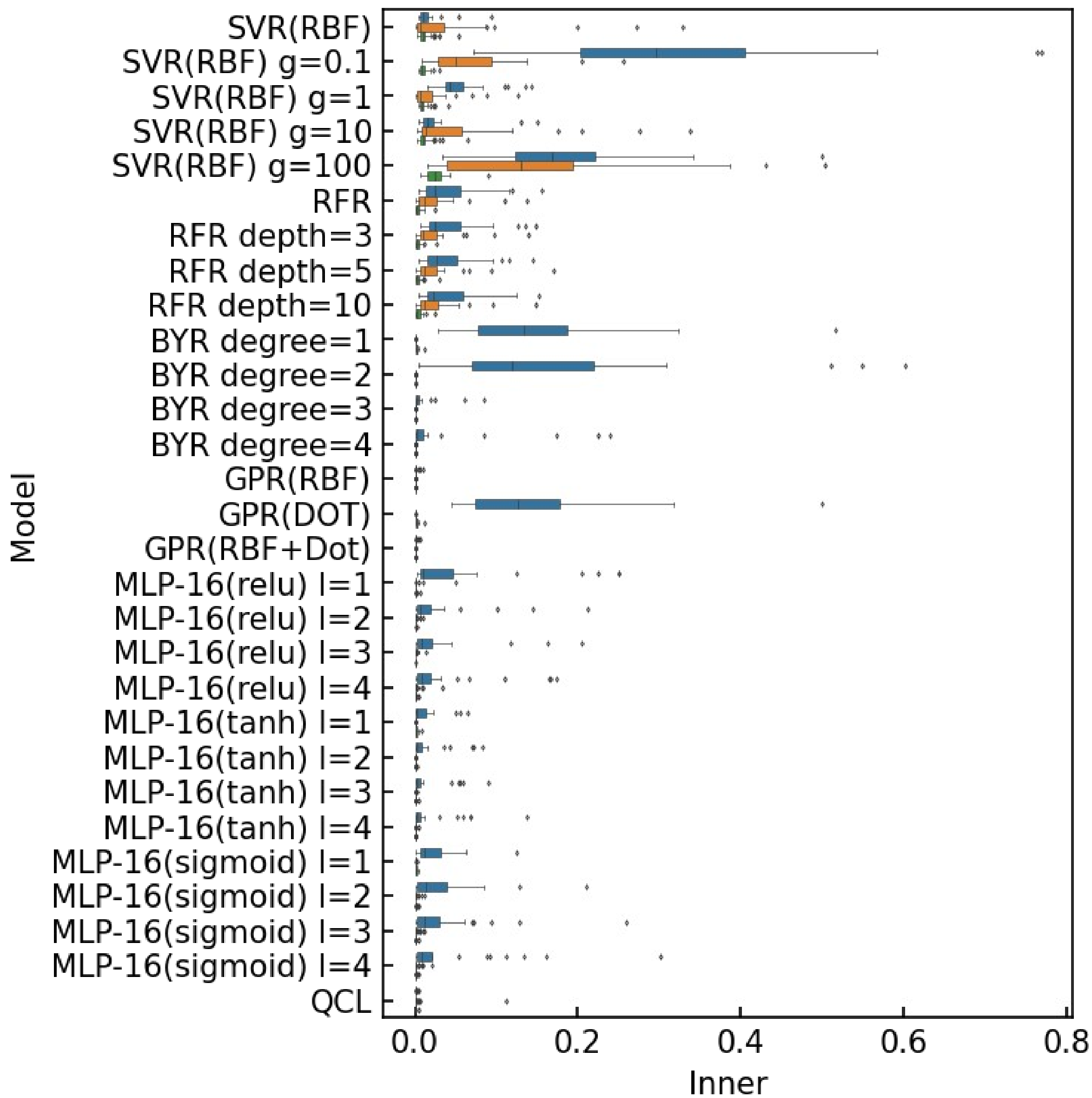
SVR(RBF)
SVR(RBF) g=0.1
SVR(RBF) g=1
SVR(RBF) g=10
SVR(RBF) g=100
RFR
RFR depth=3
RFR depth=5
RFR depth=10
BYR degree=1
BYR degree=2
BYR degree=3
BYR degree=4
GPR(RBF)
GPR(DOT)
GPR(RBF+Dot)
MLP-16(relu) l=1
MLP-16(relu) l=2
MLP-16(relu) l=3
MLP-16(relu) l=4
MLP-16(tanh) l=1
MLP-16(tanh) l=2
MLP-16(tanh) l=3
MLP-16(tanh) l=4
MLP-16(sigmoid) l=1
MLP-16(sigmoid) l=2
MLP-16(sigmoid) l=3
MLP-16(sigmoid) l=4
QCL
Model
0.0
0.2
0.4
0.6
0.8
Inner

c)

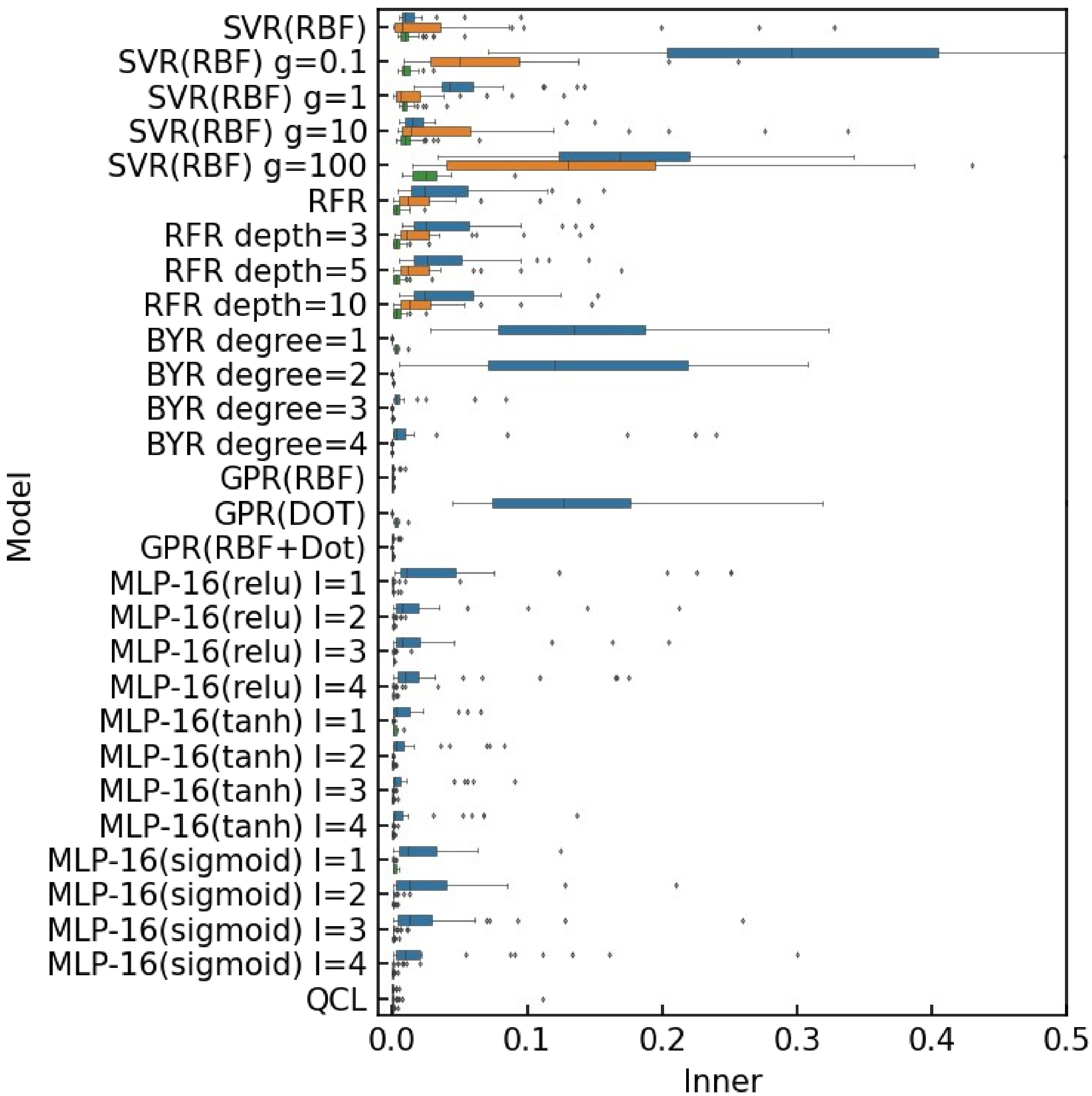

Figure S 4 Mean squared errors (MSEs) for the one-dimensional regression tasks. The random data preparation and regressions were repeated 30 times. a,b) Prediction errors for the testing datasets in the extrapolating regions and c,d) for interpolating regions. For clearer comparison, enlarged graphs are shown in Figures b and d) by setting the *x*-range of 0 to 0.5.

Table S3 Average MSEs for the regression task in Figure S 4. Extra and inner represent the testing data in the extrapolating and interpolating regions, respectively. The "Total" column is the sum of Extra (all) and Inner (all), which are average MSEs for the regression tasks of linear, sin, and exponential curves.

Model	Extra (all)	Inner (all)	Total	Extra (linear)	Inner (linear)	Extra (sin)	Inner (sin)	Extra (exp)	Inner (exp)
GPR(RBF+Dot)	0.0034	0.00018	0.0036	3.3e-11	1.2e-11	0.0096	0.00052	0.00069	2.3e-05
GPR(RBF)	0.0053	0.00027	0.0056	0.00063	6.9e-05	0.014	0.0007	0.0011	4e-05
QCL	0.02	0.0018	0.022	0.039	0.0045	0.0052	0.00037	0.017	0.00043
MLP-16(tanh) l=3	0.049	0.0042	0.054	0.002	0.00027	0.14	0.012	0.0054	0.00029
MLP-16(tanh) l=1	0.054	0.004	0.058	0.0011	0.00012	0.15	0.011	0.011	0.0013
MLP-16(tanh) l=4	0.053	0.0054	0.059	0.002	0.00031	0.15	0.016	0.0046	0.00021
MLP-16(tanh) l=2	0.054	0.0044	0.059	0.00097	9.3e-05	0.16	0.013	0.0059	0.0003
BYR degree=3	0.08	0.0029	0.083	8.3e-11	7.5e-12	0.24	0.0086	0.0001	3.3e-06
MLP-16(sigmoid) l=1	0.11	0.0079	0.12	0.0027	0.0003	0.32	0.022	0.012	0.0013
MLP-16(sigmoid) l=2	0.13	0.011	0.14	0.011	0.0013	0.37	0.03	0.0056	0.00042
MLP-16(sigmoid) l=3	0.13	0.011	0.14	0.015	0.0017	0.37	0.032	0.0071	0.0004
MLP-16(sigmoid) l=4	0.13	0.013	0.15	0.018	0.0021	0.37	0.037	0.0075	0.00038
MLP-16(relu) l=3	0.16	0.009	0.17	0.012	0.00095	0.45	0.026	0.0048	0.00037
MLP-16(relu) l=2	0.16	0.0088	0.17	0.0084	0.001	0.46	0.025	0.0031	0.00026
MLP-16(relu) l=4	0.16	0.011	0.17	0.014	0.0021	0.45	0.031	0.0052	0.0006
SVR(RBF)	0.15	0.024	0.18	0.31	0.044	0.062	0.015	0.078	0.013
RFR	0.17	0.022	0.2	0.13	0.023	0.35	0.039	0.038	0.0043
RFR depth=3	0.18	0.023	0.2	0.13	0.023	0.36	0.041	0.038	0.0043
RFR depth=10	0.18	0.023	0.2	0.13	0.024	0.36	0.041	0.038	0.0043
RFR depth=5	0.18	0.023	0.2	0.13	0.024	0.36	0.04	0.038	0.0043
SVR(RBF) g=10	0.18	0.031	0.21	0.42	0.056	0.032	0.024	0.093	0.013
SVR(RBF) g=1	0.2	0.028	0.23	0.15	0.019	0.39	0.055	0.058	0.011
MLP-16(relu) l=1	0.25	0.018	0.27	0.017	0.0024	0.72	0.05	0.0066	0.00048
BYR degree=4	0.28	0.0093	0.29	8.2e-08	1.1e-08	0.84	0.028	1.7e-05	2.6e-07
SVR(RBF) g=0.1	0.17	0.13	0.3	0.19	0.067	0.26	0.33	0.048	0.01
SVR(RBF) g=100	0.31	0.12	0.43	0.73	0.15	0.071	0.18	0.14	0.026
GPR(DOT)	0.43	0.048	0.48	2.2e-11	7.6e-12	1.3	0.14	0.022	0.0028
BYR degree=1	0.46	0.049	0.5	2e-14	7.8e-15	1.3	0.14	0.022	0.0028
BYR degree=2	0.77	0.057	0.83	2e-12	4.3e-13	2.3	0.17	0.0016	0.00011

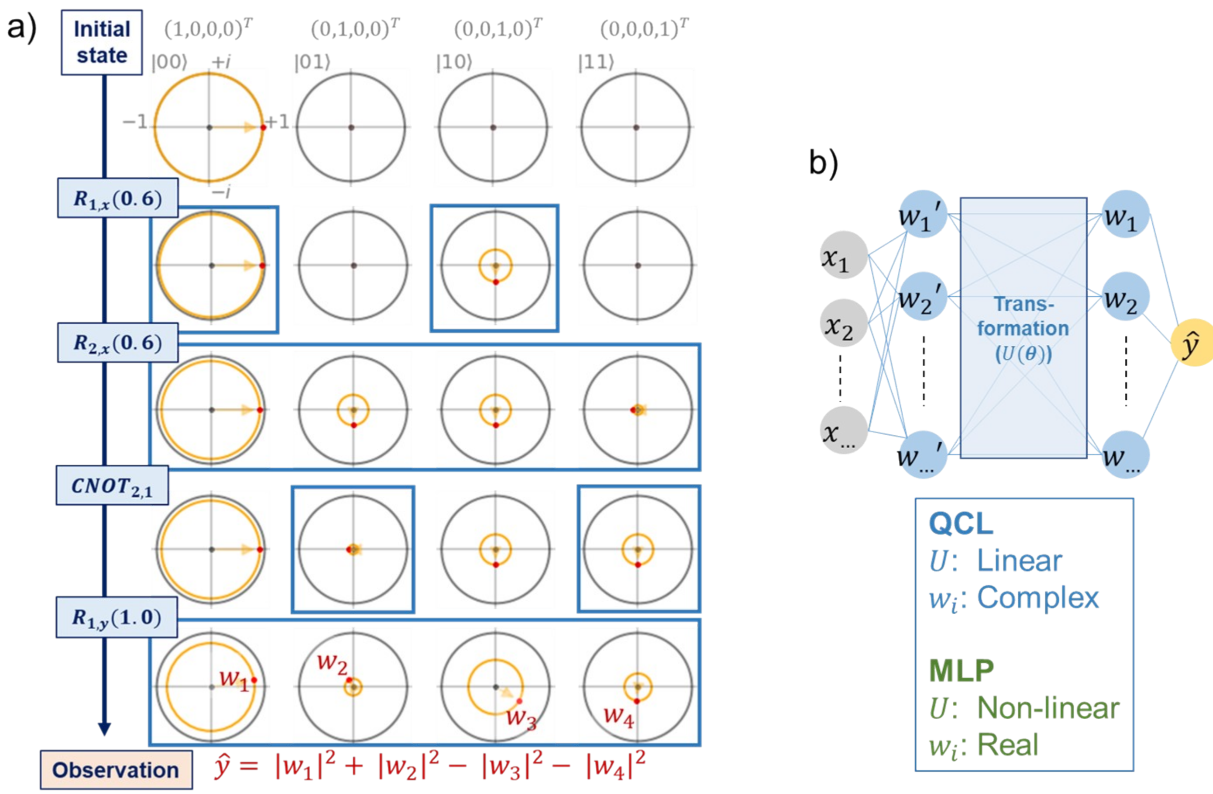

Figure S 5 a) Visualized state vector for an example circuit of $U(\theta)V(x) = R_{1,y}(\theta) \cdot CNOT_{1,2} \cdot R_{2,x}(x) \cdot R_{1,x}(x)$ ($\theta = 1.0, x = 0.6$). Coordinate w_i against four bases $|00\rangle = (1,0,0,0)^T,\ldots,|11\rangle = (0,0,0,1)^T$ are plotted as red points on complex planes. Changes of w_i by gates are marked by blue squares. b) Model design of QCL and MLP.

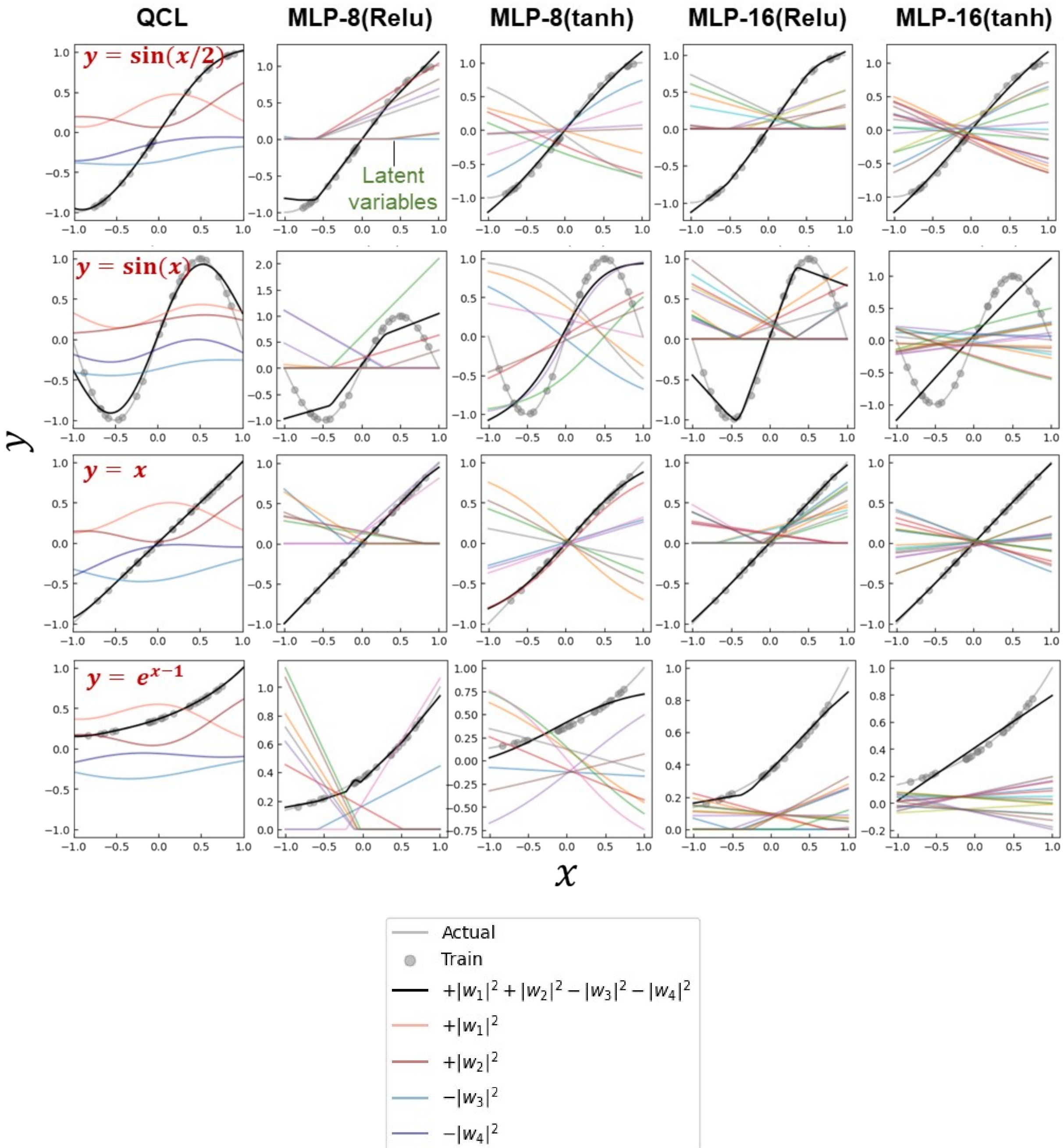

Figure S 6 Visualization of latent variables for the QCL and MLP models. Gray plots and lines show answer data, black lines correspond to final predictions, and other colored curves are latent variables. The expression of “MLP-8(ReLu)” represents that an 8-dimensional hidden layer and a ReLu activation function were selected as hyperparameters. Related data is shown in Figure 5.

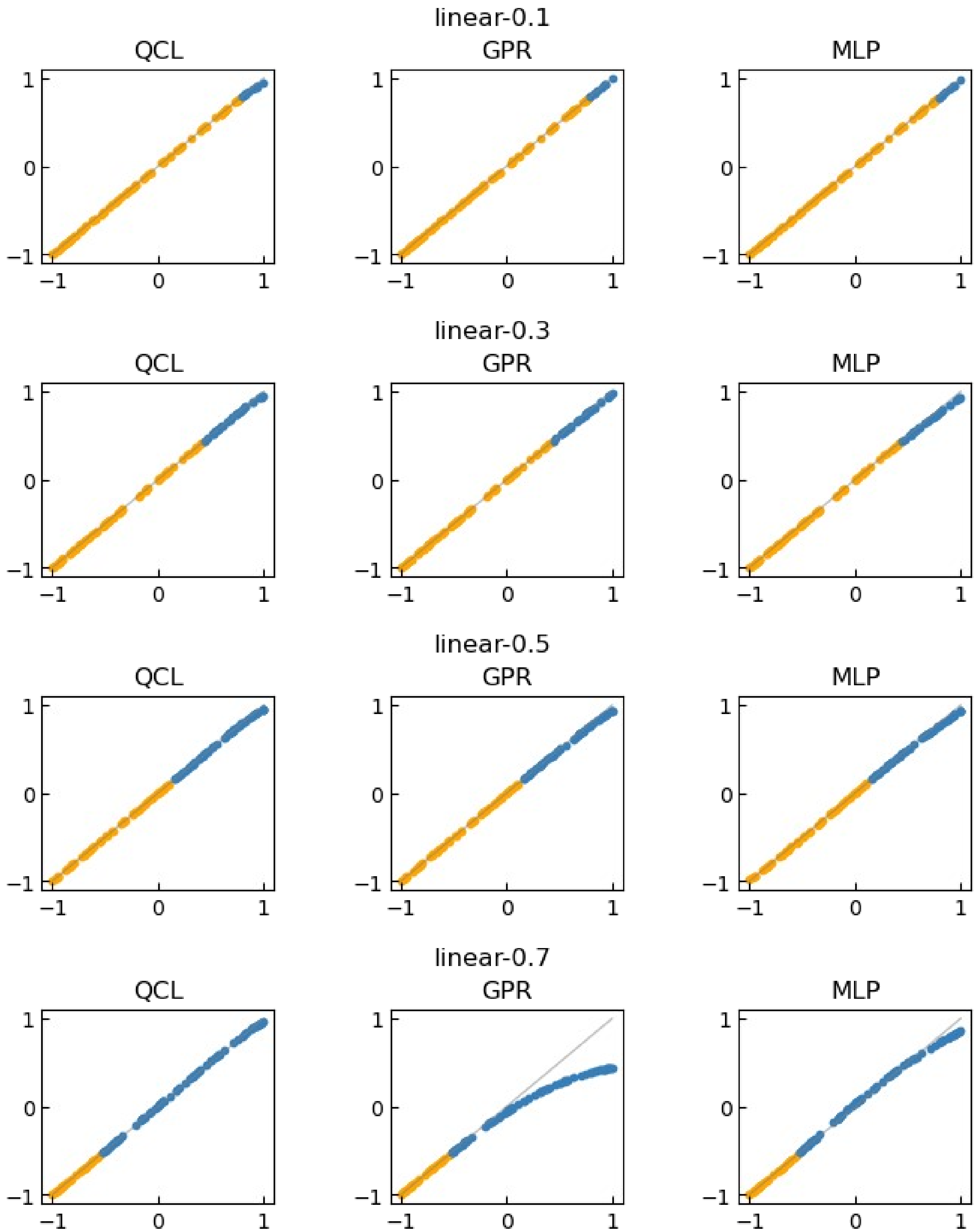
linear-0.1
QCL
GPR
MLP
linear-0.3
QCL
GPR
MLP
linear-0.5
QCL
GPR
MLP
linear-0.7
QCL
GPR
MLP

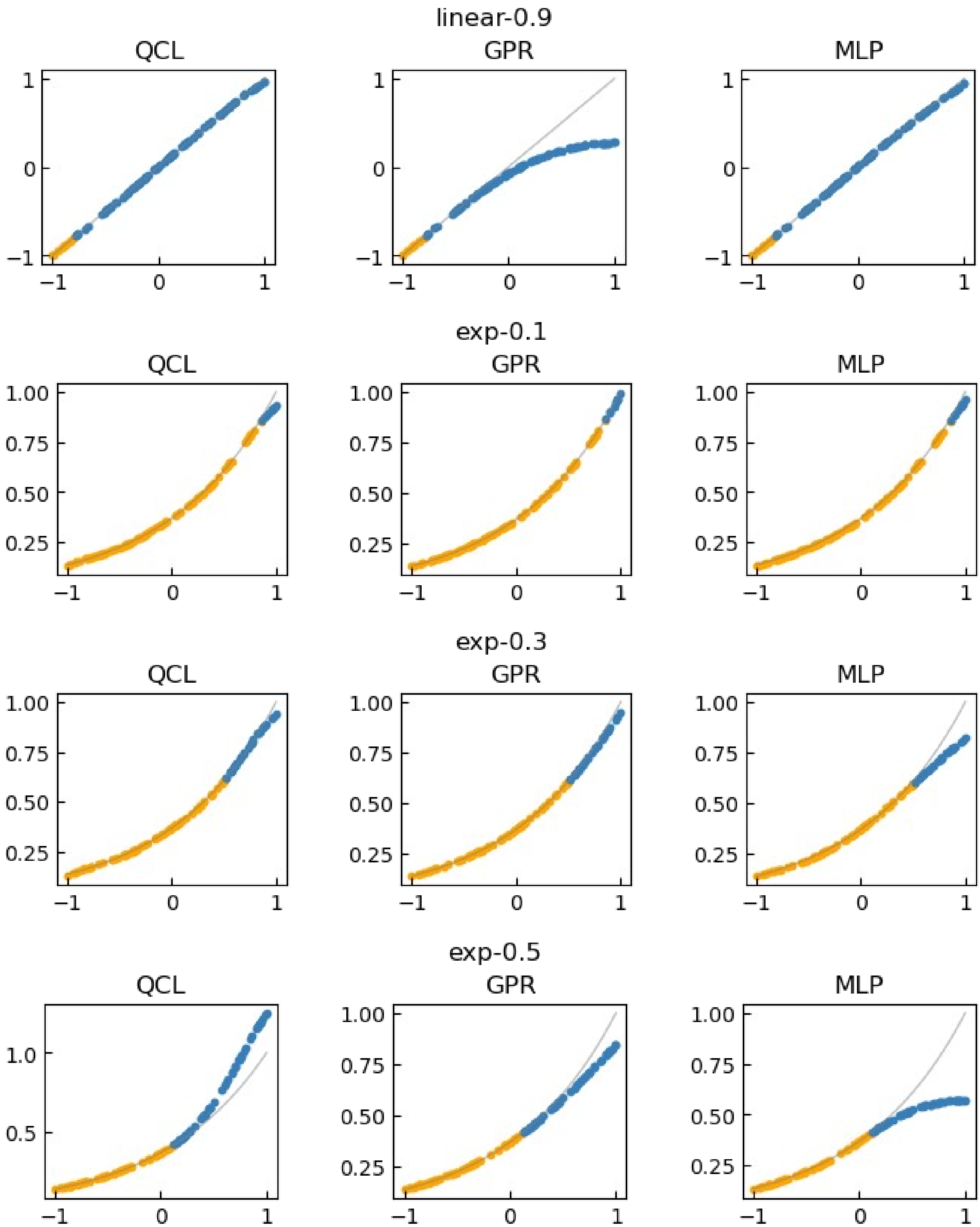
linear-0.9
QCL
GPR
MLP
exp-0.1
QCL
GPR
MLP
exp-0.3
QCL
GPR
MLP
exp-0.5
QCL
GPR
MLP

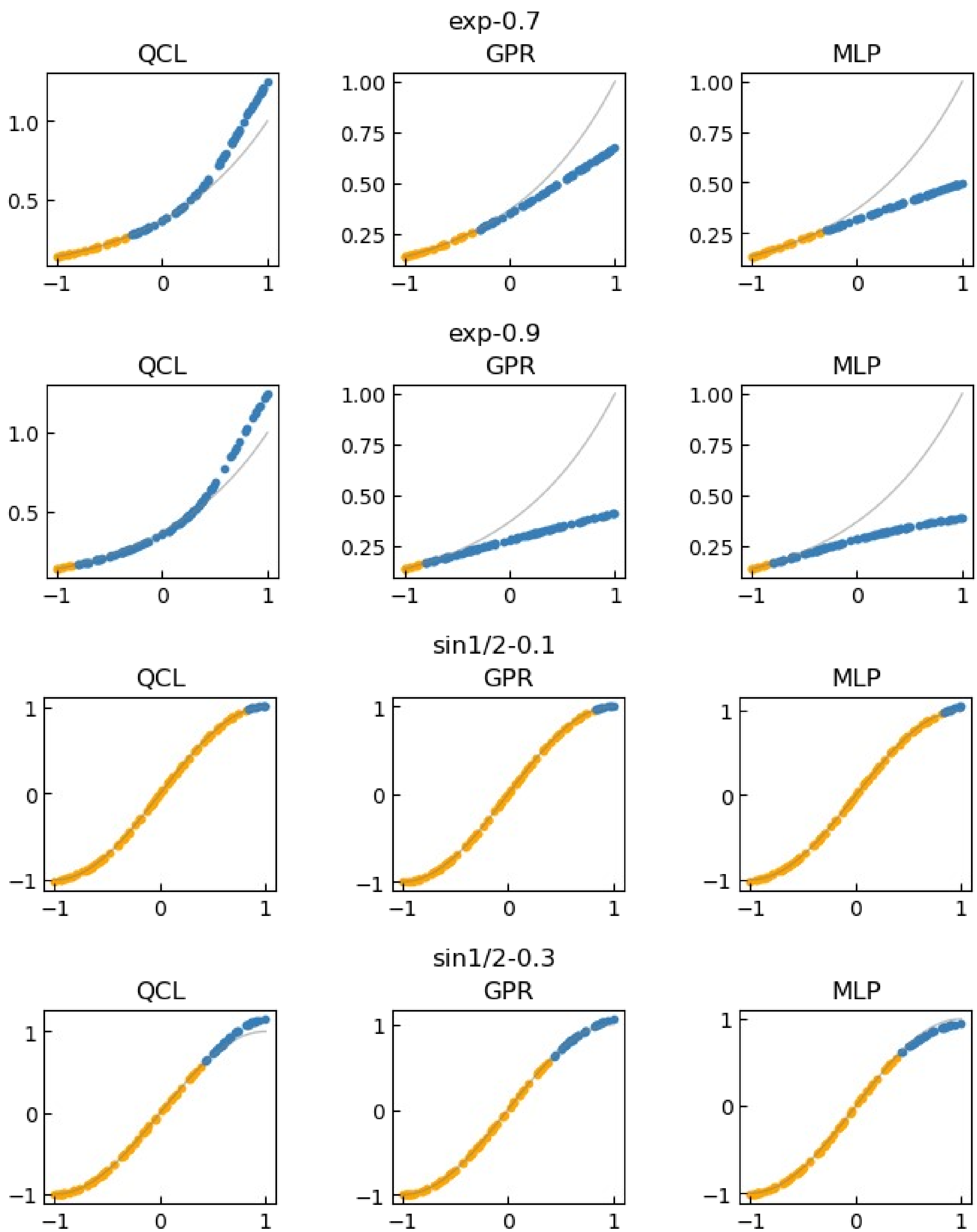
exp-0.7
QCL
GPR
MLP
exp-0.9
QCL
GPR
MLP
sin1/2-0.1
QCL
GPR
MLP
sin1/2-0.3
QCL
GPR
MLP

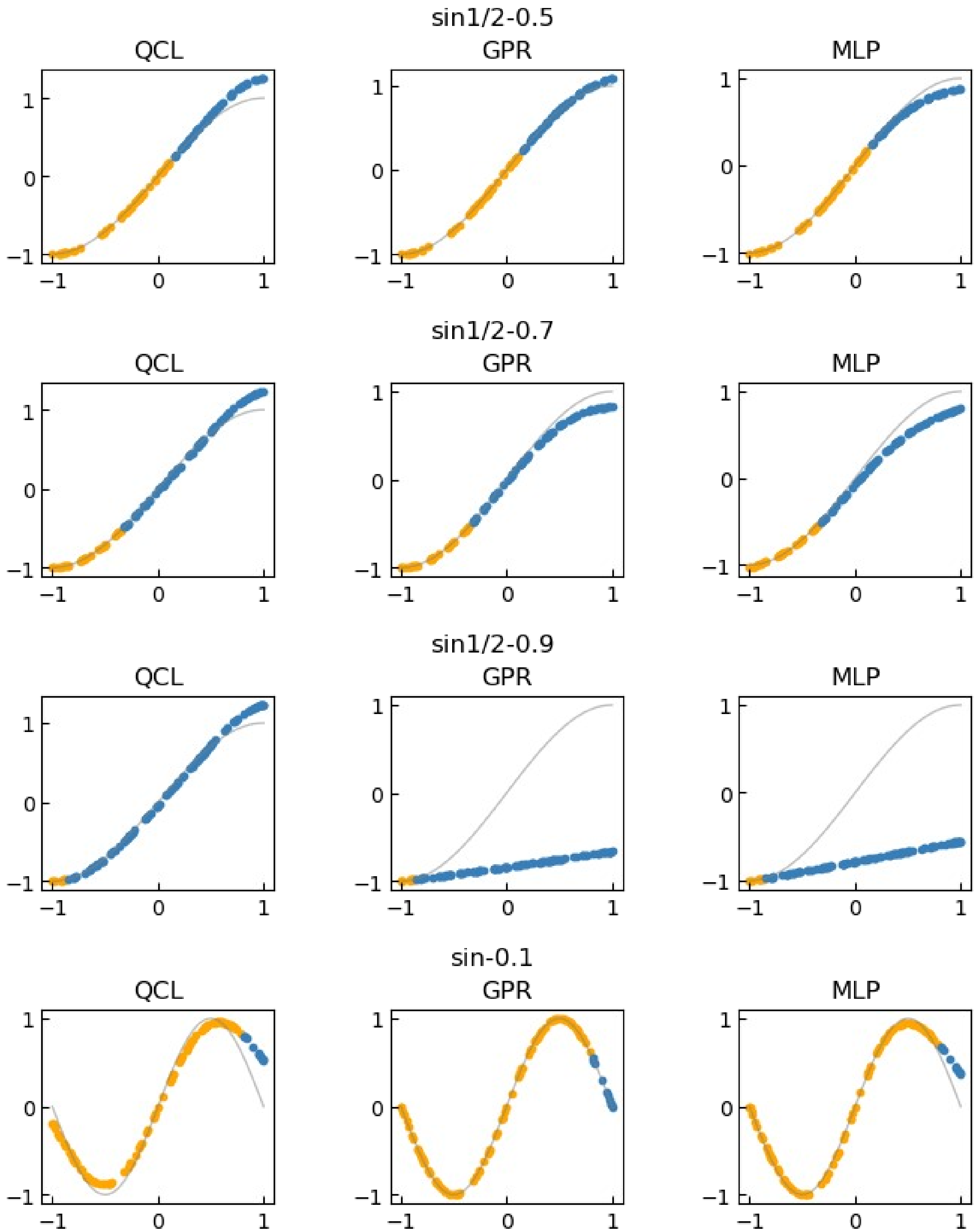

sin1/2-0.5
QCL
GPR
MLP
sin1/2-0.7
QCL
GPR
MLP
sin1/2-0.9
QCL
GPR
MLP
sin-0.1
QCL
GPR
MLP

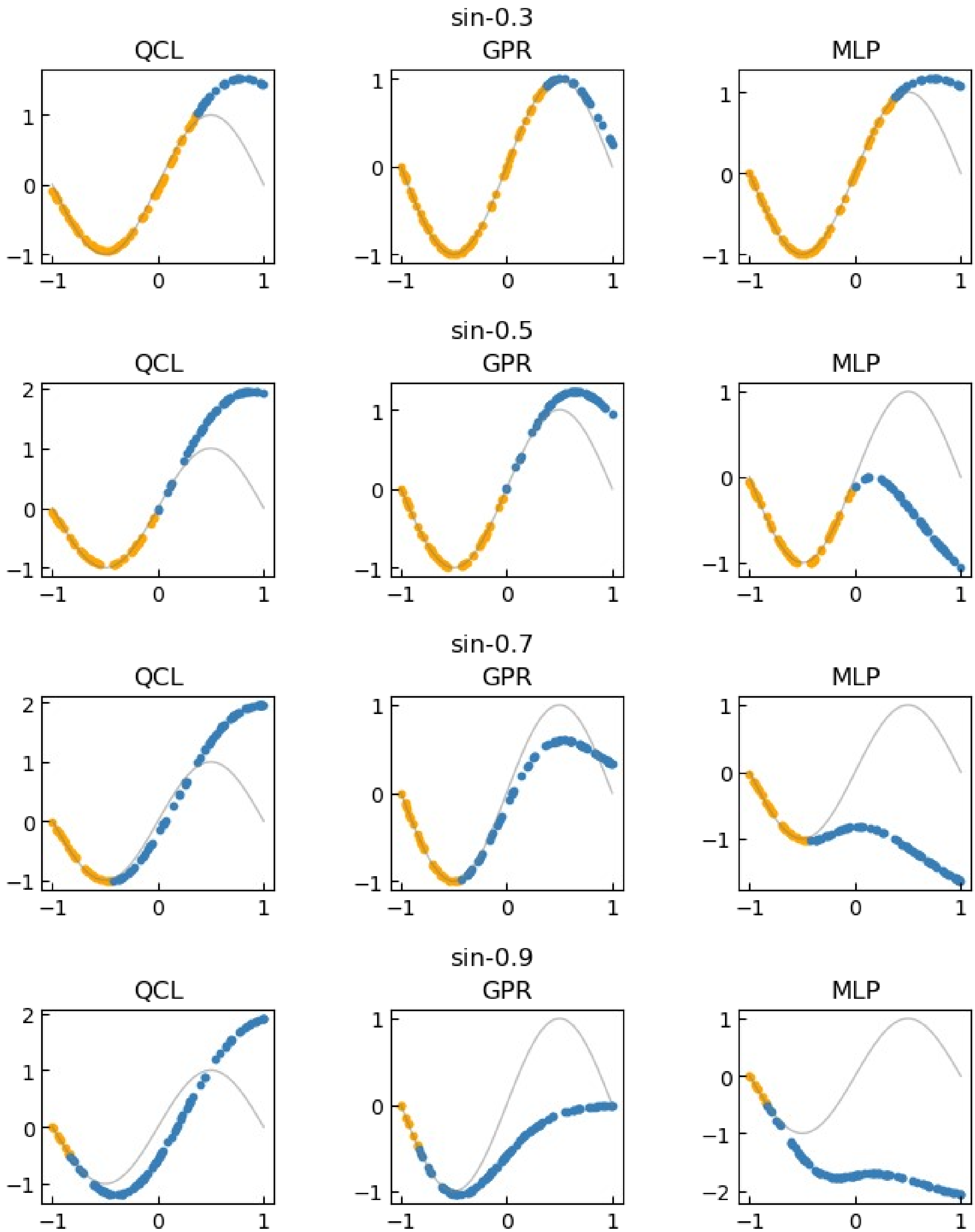
sin-0.3
QCL
GPR
MLP
sin-0.5
QCL
GPR
MLP
sin-0.7
QCL
GPR
MLP
sin-0.9
QCL
GPR
MLP
−1
0
1
2
−2

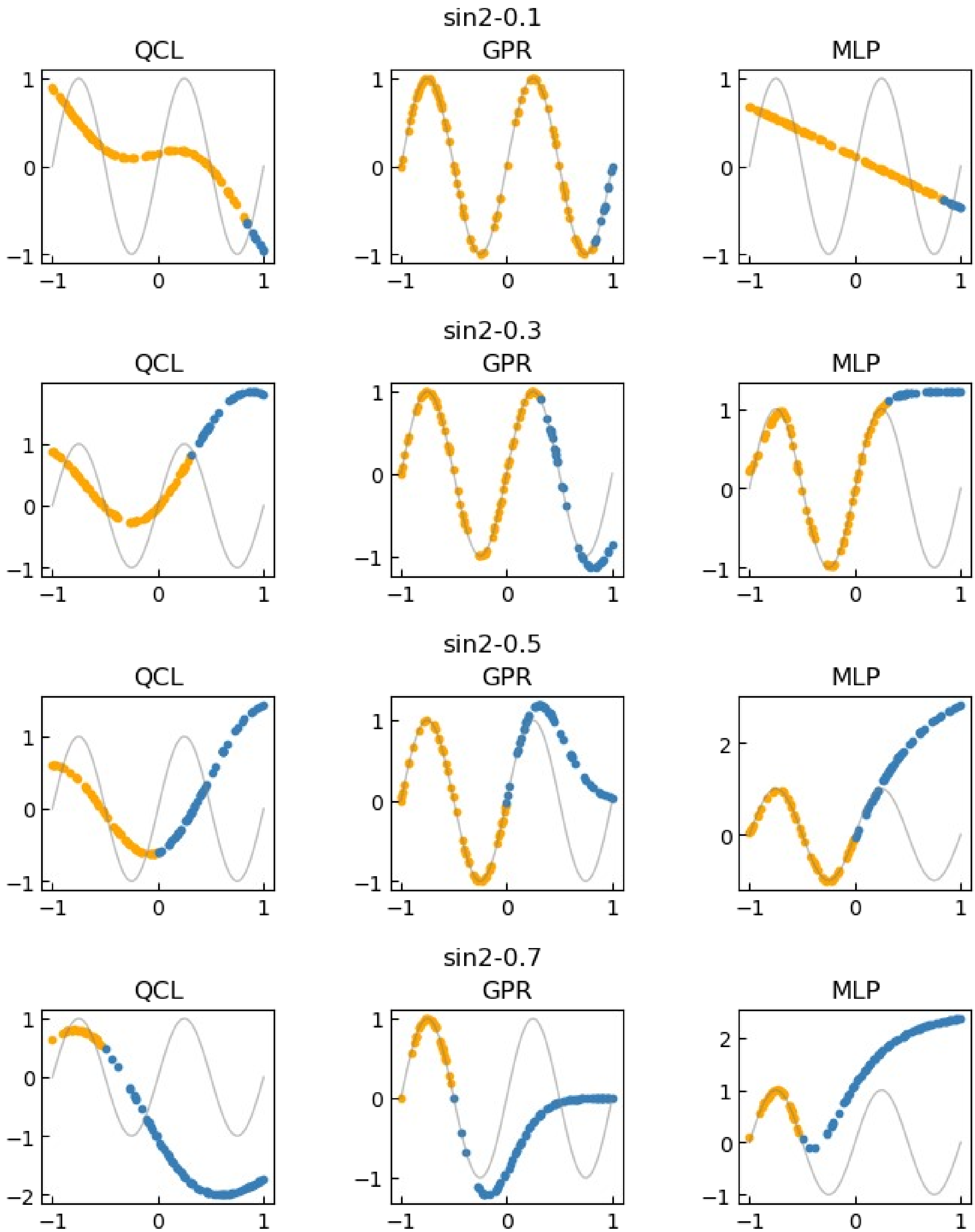
sin2-0.1
QCL
GPR
MLP
sin2-0.3
QCL
GPR
MLP
sin2-0.5
QCL
GPR
MLP
sin2-0.7
QCL
GPR
MLP

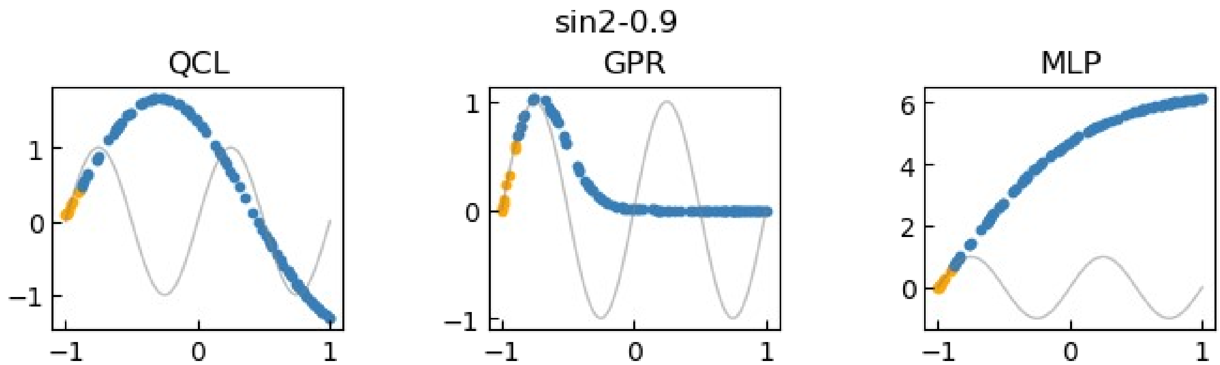

Figure S 7 Extrapolating predictions of linear, exponential, and sinusoidal functions by QCL, GPR (RBF), and MLP-8. Random 100 points were generated according to the original functions. Extrapolating 10, 30, 50, 70, or 90% of the data were selected as testing sets, and the rest were training. The expression of, e.g., "sin2-0.9" indicates that a $\sin 2x$ function was fitted with the 90% extrapolating testing data.

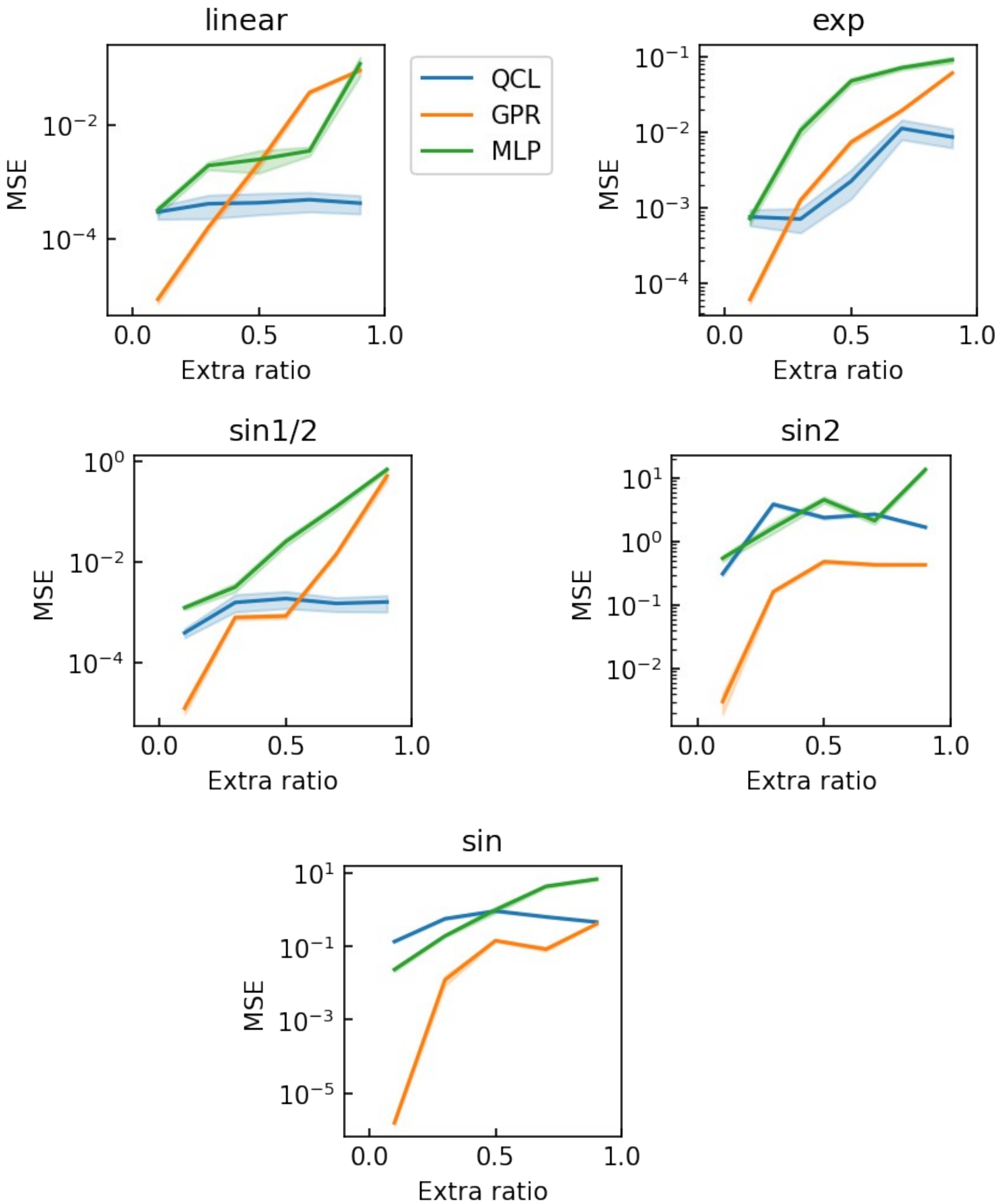

Figure S 8 Statistical extrapolating performances for Figure S 7. The random dataset preparation and fitting were repeated 30 times. Transparent regions show standard errors with 68% confidence intervals.

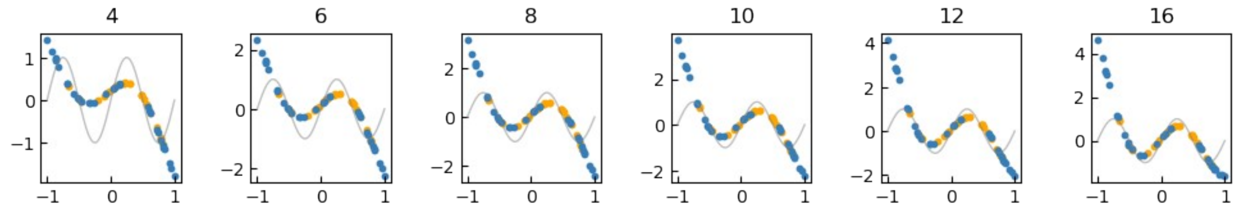

Figure S 9 Regression of $sin(2x)$ by normal QCL models with different prefactors for observable ($\hat{y} \mapsto c\hat{y}$, $c = 4,6,8,10,12, or\ 16$). The increase of the constant enabled the better fitting of $sin(2x)$ in the inner region. However, prediction errors in the extrapolating areas became much larger.

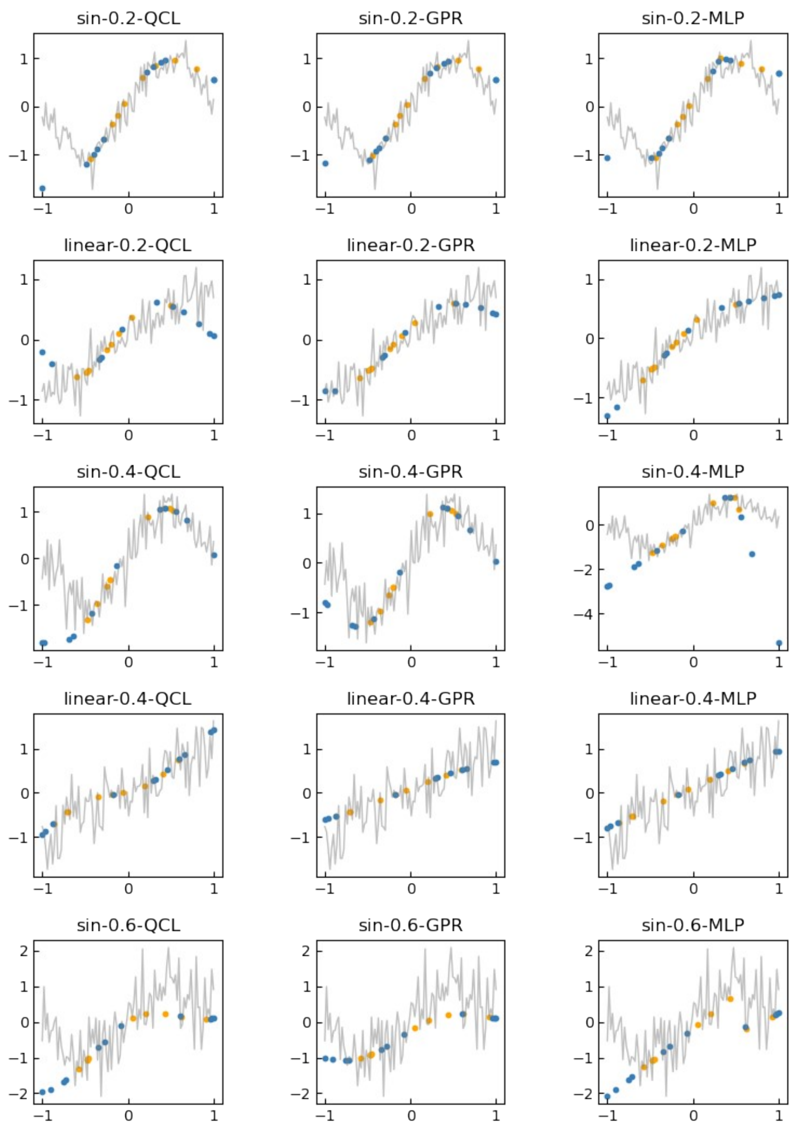

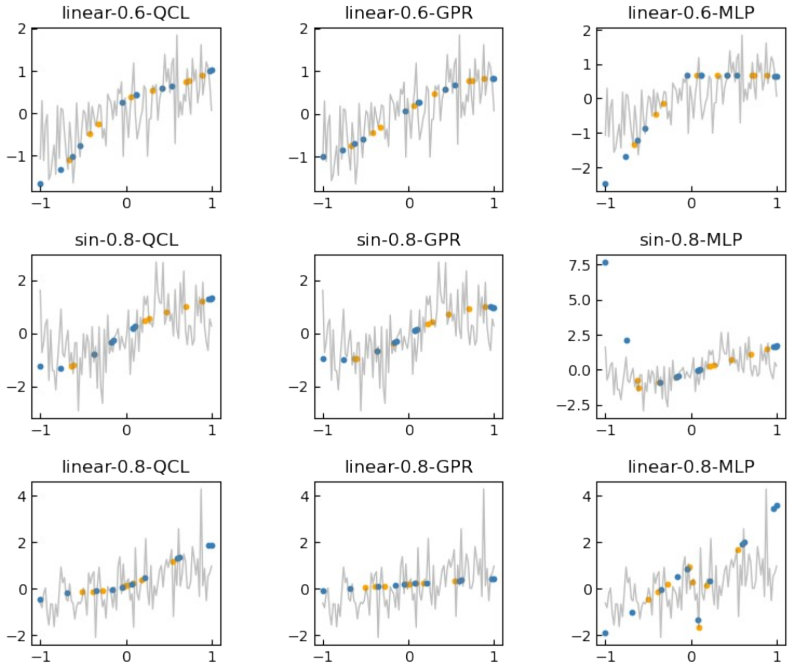

Figure S 10 Regression of noised $\sin(x)$ or x by normal QCL, GPR, MLP-8 models. An expression of sin-z-QCL means that Gaussian random noises were added to a sinusoidal curve with a scaling factor of z.

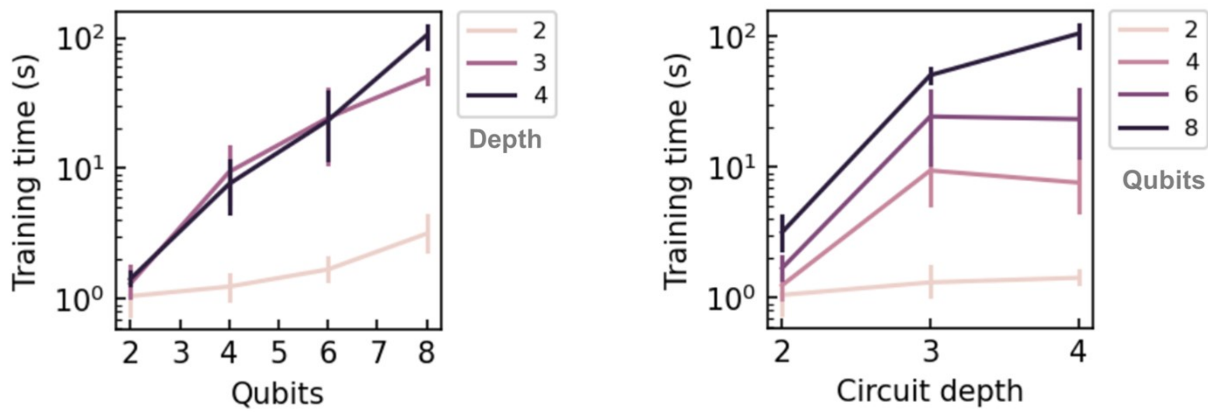

Figure S 11 Training time of QCL model (configuration shown in Figure 3b). The number of qubits n and circuit depth m were changed to train random 50 records of $y = \sin(x)$. Predictions were done by calculating from state vectors and repeated five times for each condition. Error bars indicate 95% confidence intervals assuming Gaussian distribution.

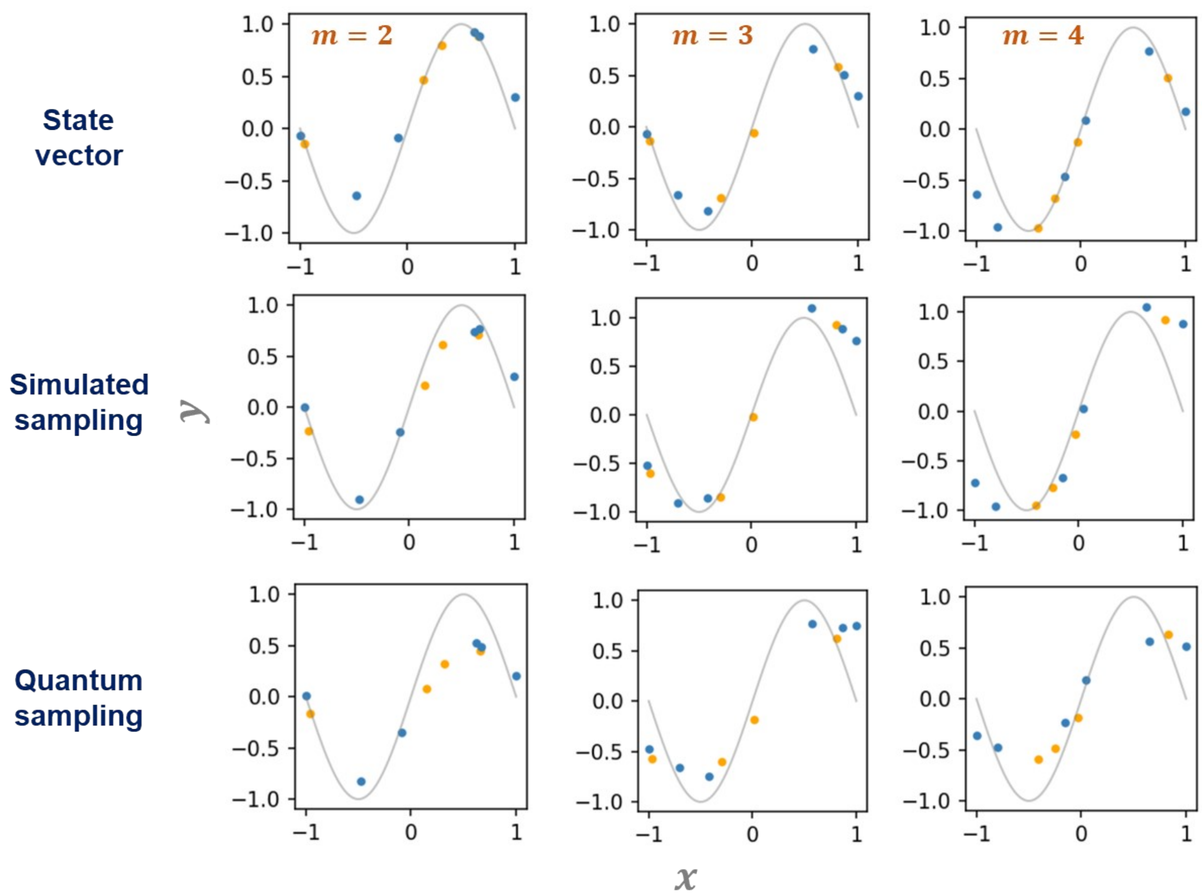

Figure S 12 Predicting the function of $y = \sin(x)$ by an actual quantum computer (IBM Quantum) with $m = 2, 3, or\ 4$. Models were trained using the output of state vectors. Then, simulated or actual quantum computations were conducted to predict the same data from sampling results (**Eq 7**). For one record, sampling was done 1000 times. The accuracy of simulated sampling was worse than the state vector due to the randomness. Worse results of quantum sampling than simulation meant that noises during quantum computing affected the predictions.

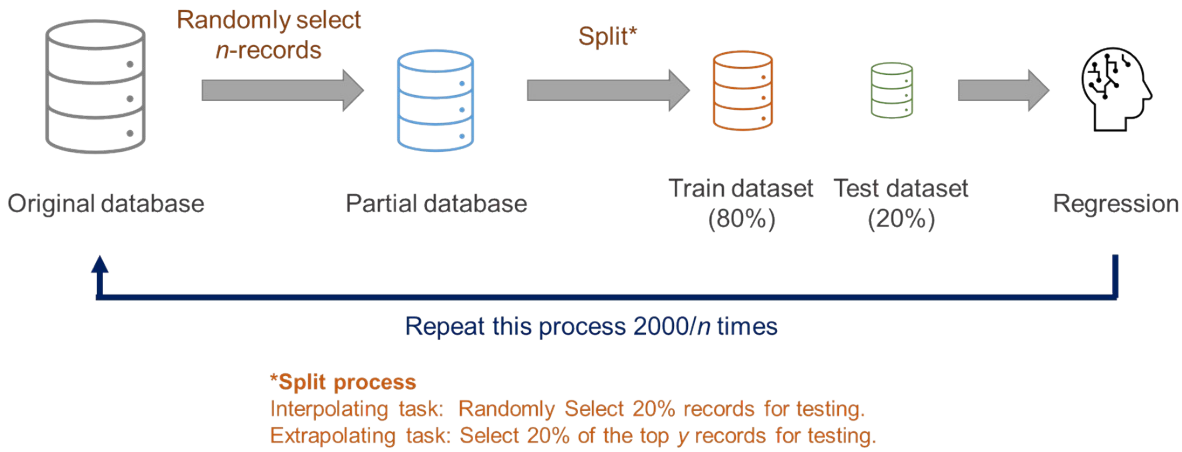

Figure S 13 Dataset preparation and regression steps for the molecular property prediction task. The dataset size of n was set to be 8, 16, 32, 64, 128, 256, or 512.

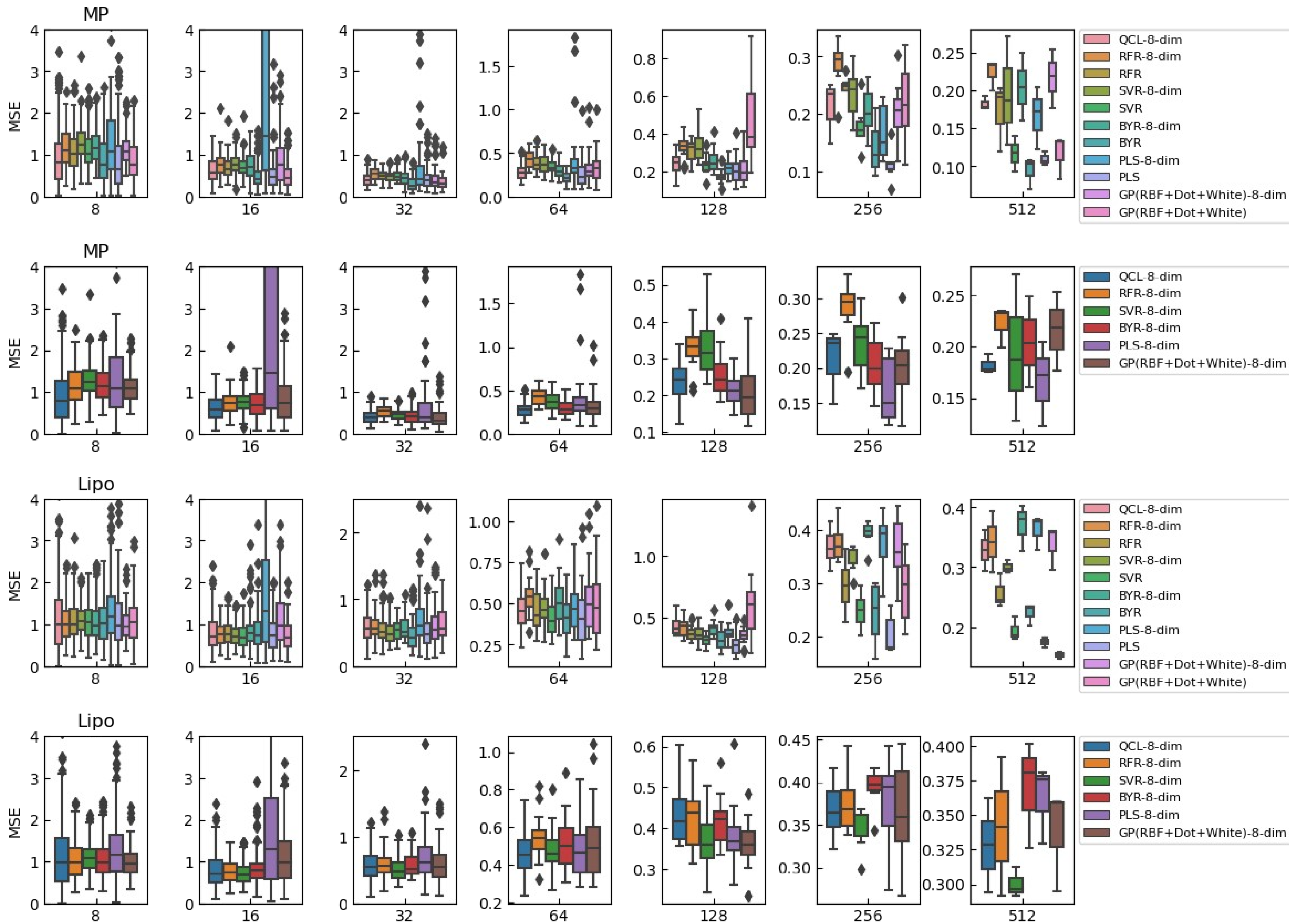

MP
MP
Lipo
Lipo
MSE
8
16
32
64
128
256
512
QCL-8-dim
RFR-8-dim
RFR
SVR-8-dim
SVR
BYR-8-dim
BYR
PLS-8-dim
PLS
GP(RBF+Dot+White)-8-dim
GP(RBF+Dot+White)

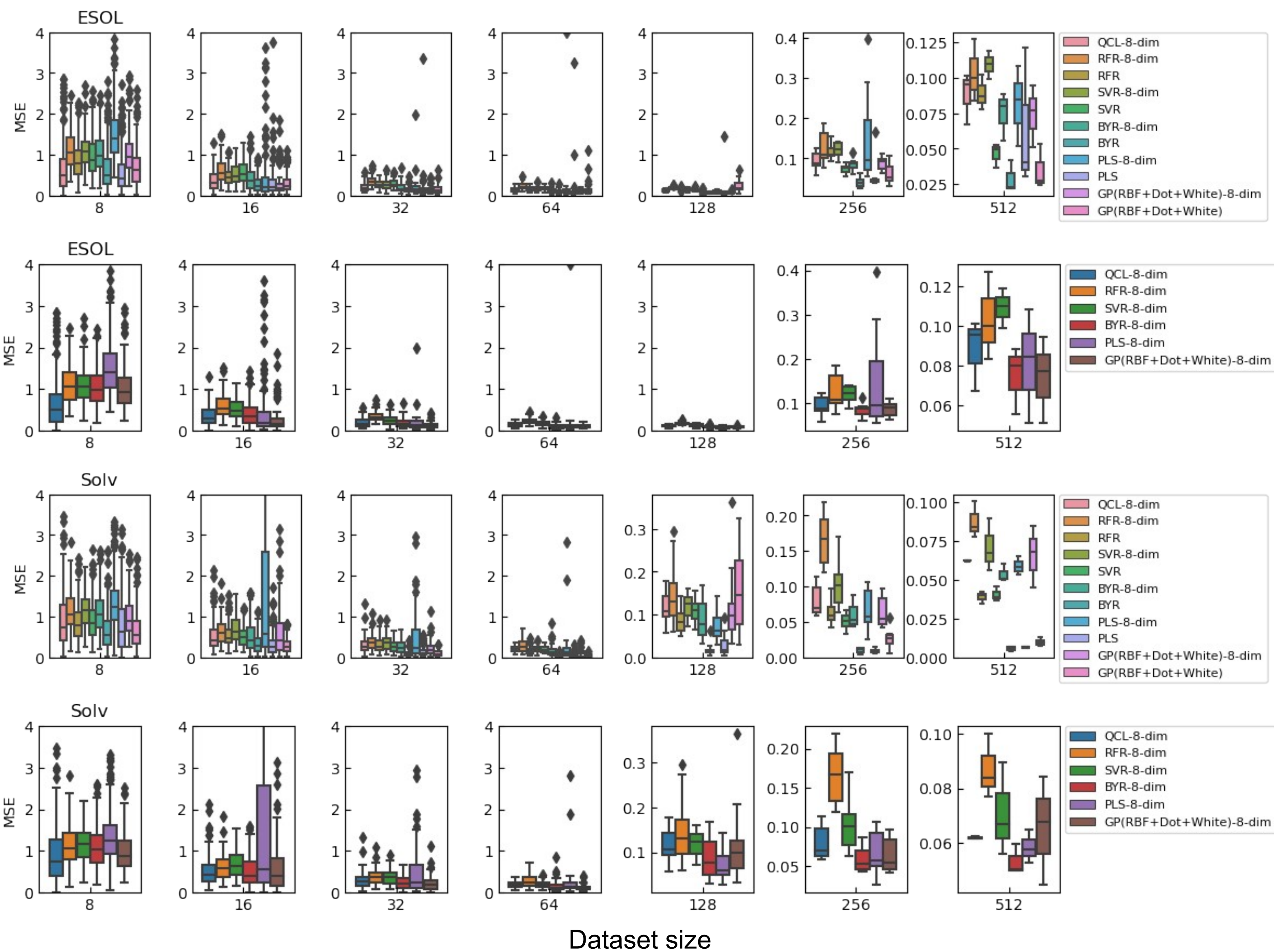
ESOL
Solv
MSE
QCL-8-dim
RFR-8-dim
RFR
SVR-8-dim
SVR
BYR-8-dim
BYR
PLS-8-dim
PLS
GP(RBF+Dot+White)-8-dim
GP(RBF+Dot+White)
8
16
32
64
128
256
512
Dataset size

a)

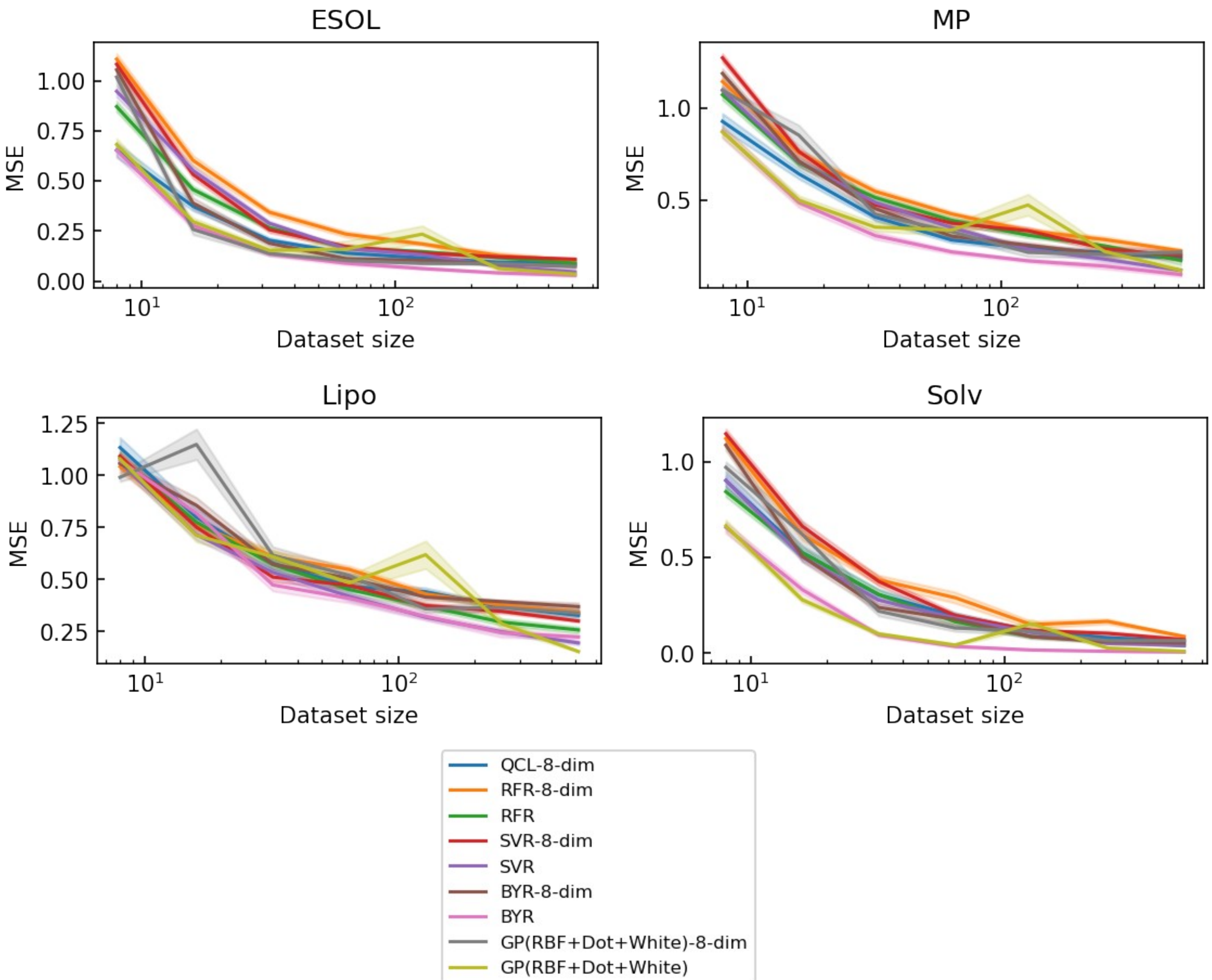

ESOL
MP
Lipo
Solv
MSE
Dataset size
QCL-8-dim
RFR-8-dim
RFR
SVR-8-dim
SVR
BYR-8-dim
BYR
GP(RBF+Dot+White)-8-dim
GP(RBF+Dot+White)

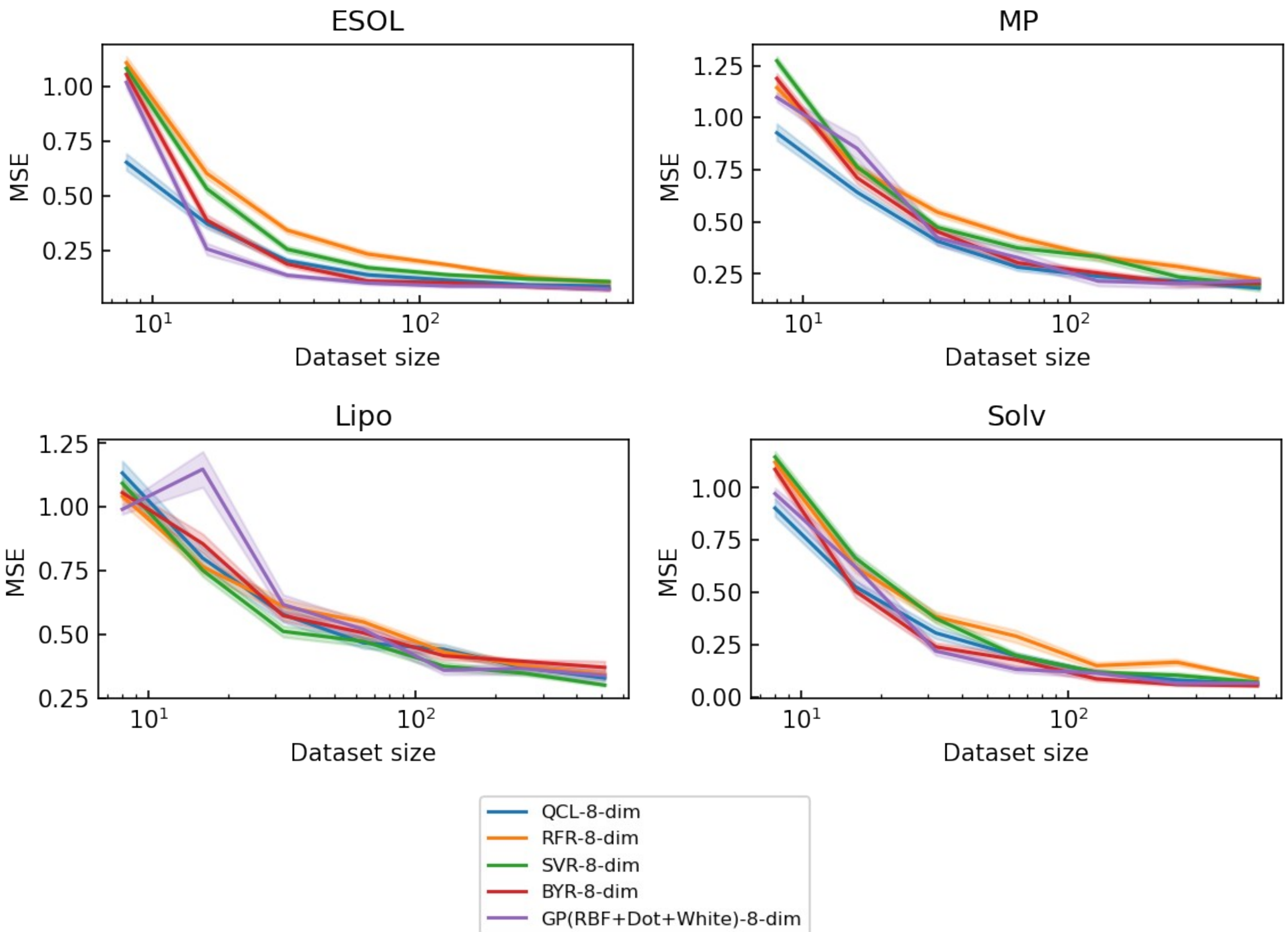

b)

Figure S 14 Regression results for the extrapolating tasks, with lipophilicity (Lipo), hydration free energy of small molecules in water (Solv), log solubility in water (ESOL), and melting point (MP) datasets. a) Box plots. b) Line plots with standard errors with 68%

confidence intervals. In the legends, “8-dim” means that the explanatory variables were compressed from about 200- to 8-dimensional by principal component analysis.

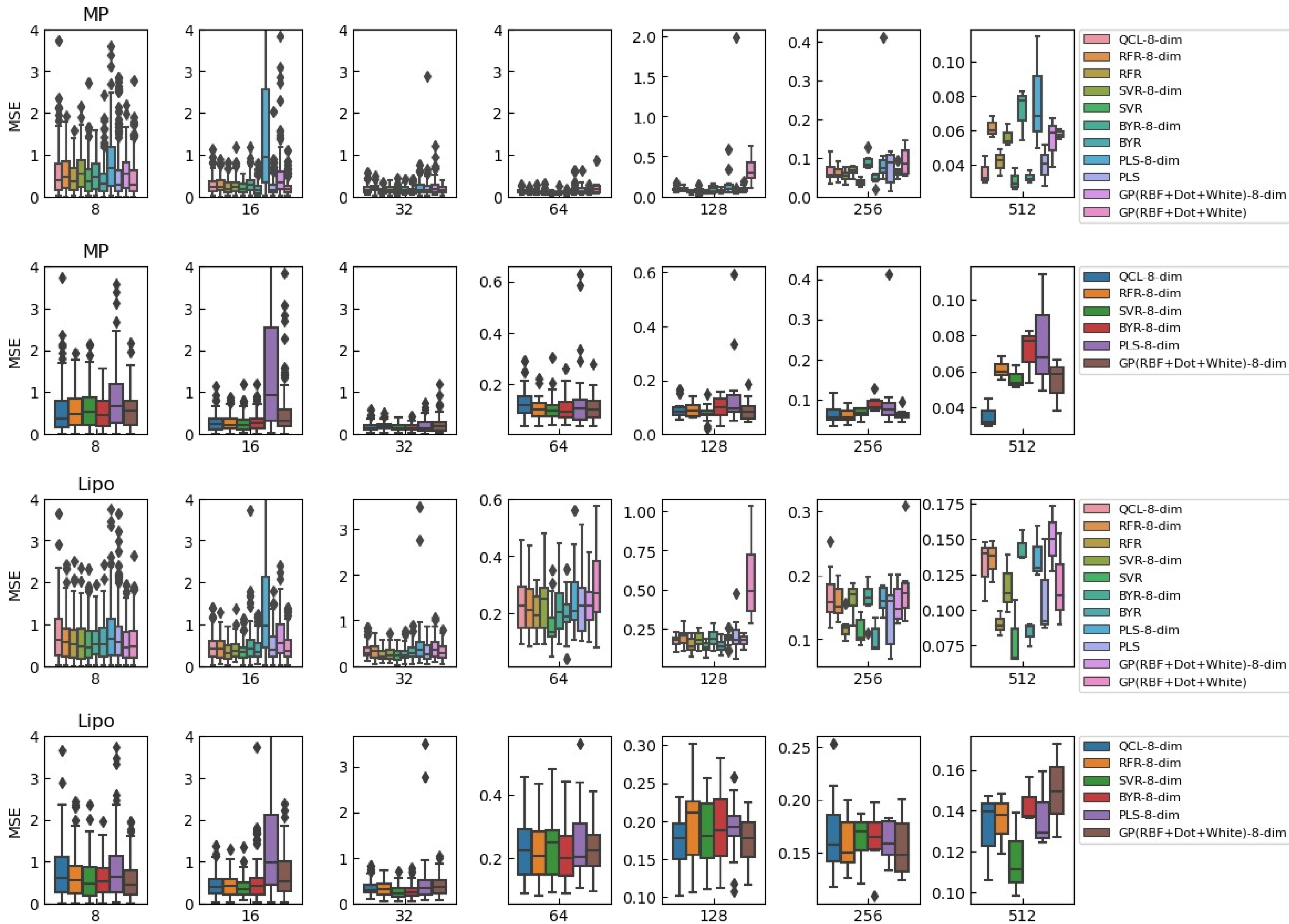
MP
MSE
8
16
32
64
128
256
512
QCL-8-dim
RFR-8-dim
RFR
SVR-8-dim
SVR
BYR-8-dim
BYR
PLS-8-dim
PLS
GP(RBF+Dot+White)-8-dim
GP(RBF+Dot+White)
MP
MSE
8
16
32
64
128
256
512
QCL-8-dim
RFR-8-dim
SVR-8-dim
BYR-8-dim
PLS-8-dim
GP(RBF+Dot+White)-8-dim
Lipo
MSE
8
16
32
64
128
256
512
QCL-8-dim
RFR-8-dim
RFR
SVR-8-dim
SVR
BYR-8-dim
BYR
PLS-8-dim
PLS
GP(RBF+Dot+White)-8-dim
GP(RBF+Dot+White)
Lipo
MSE
8
16
32
64
128
256
512
QCL-8-dim
RFR-8-dim
SVR-8-dim
BYR-8-dim
PLS-8-dim
GP(RBF+Dot+White)-8-dim

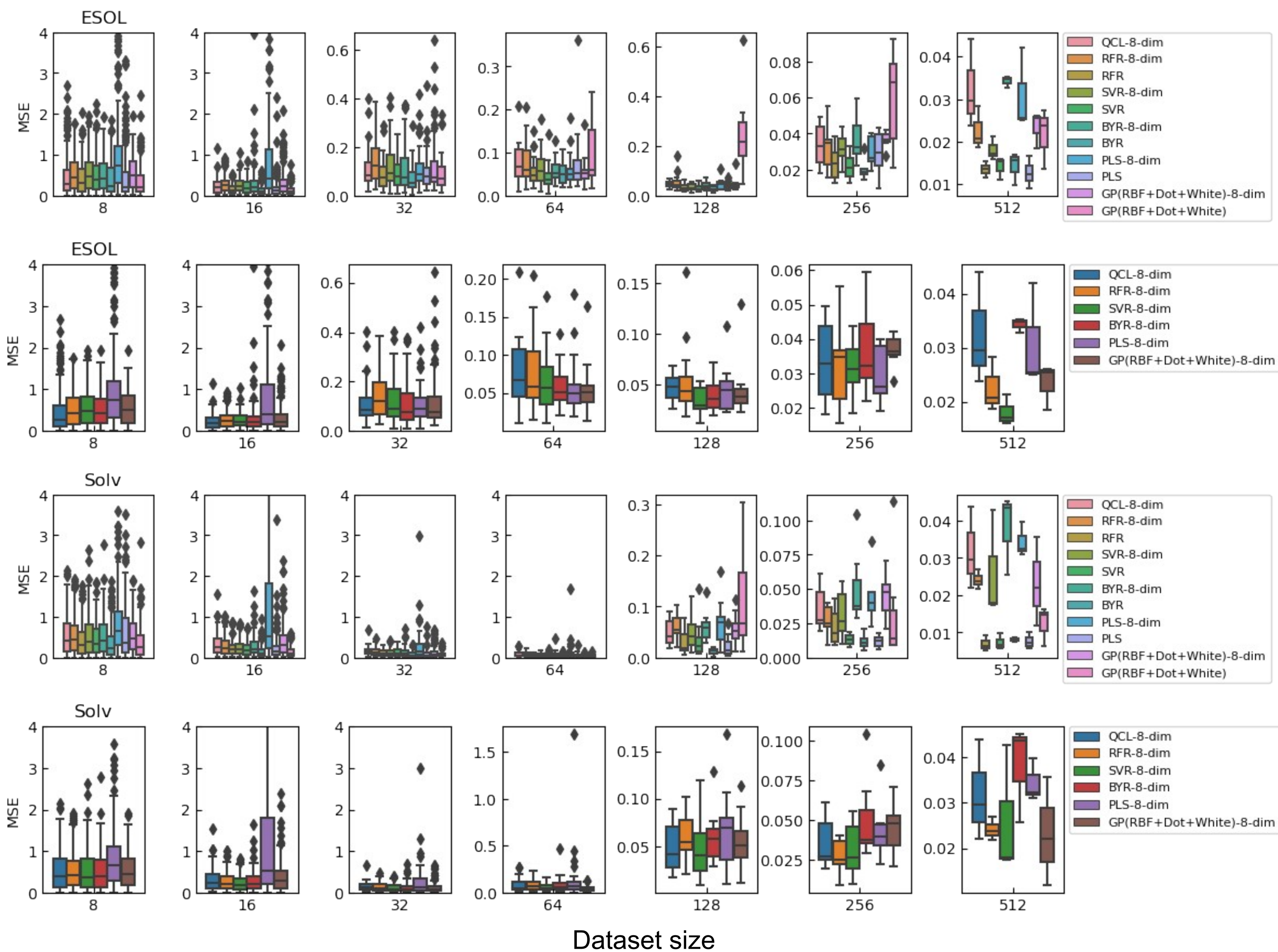
ESOL
MSE
8
16
32
64
128
256
512
QCL-8-dim
RFR-8-dim
RFR
SVR-8-dim
SVR
BYR-8-dim
BYR
PLS-8-dim
PLS
GP(RBF+Dot+White)-8-dim
GP(RBF+Dot+White)
ESOL
QCL-8-dim
RFR-8-dim
SVR-8-dim
BYR-8-dim
PLS-8-dim
GP(RBF+Dot+White)-8-dim
Solv
Solv
Dataset size

a)

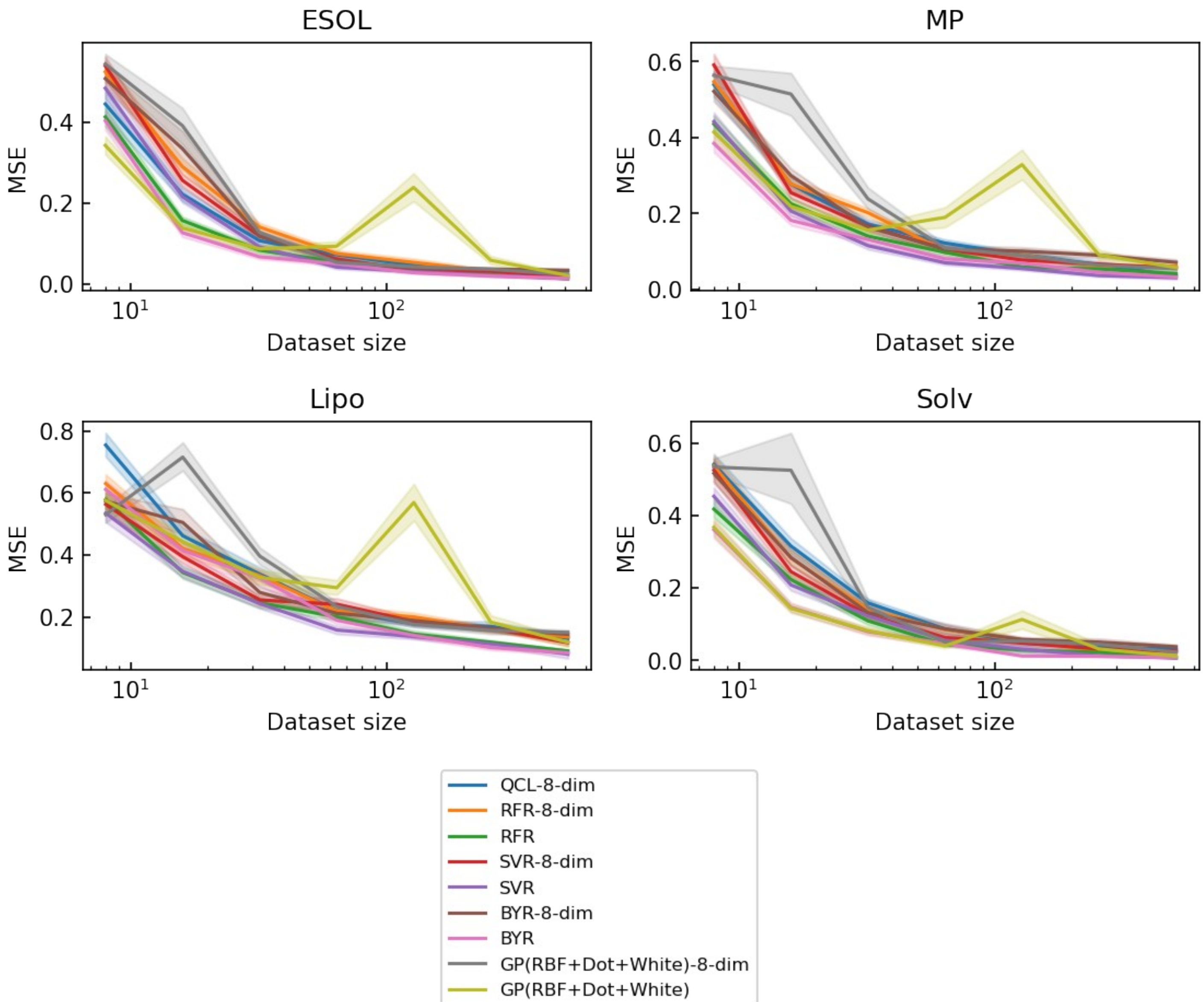
ESOL
MP
Lipo
Solv
MSE
Dataset size
0.0
0.2
0.4
0.6
0.8
10^1
10^2
QCL-8-dim
RFR-8-dim
RFR
SVR-8-dim
SVR
BYR-8-dim
BYR
GP(RBF+Dot+White)-8-dim
GP(RBF+Dot+White)

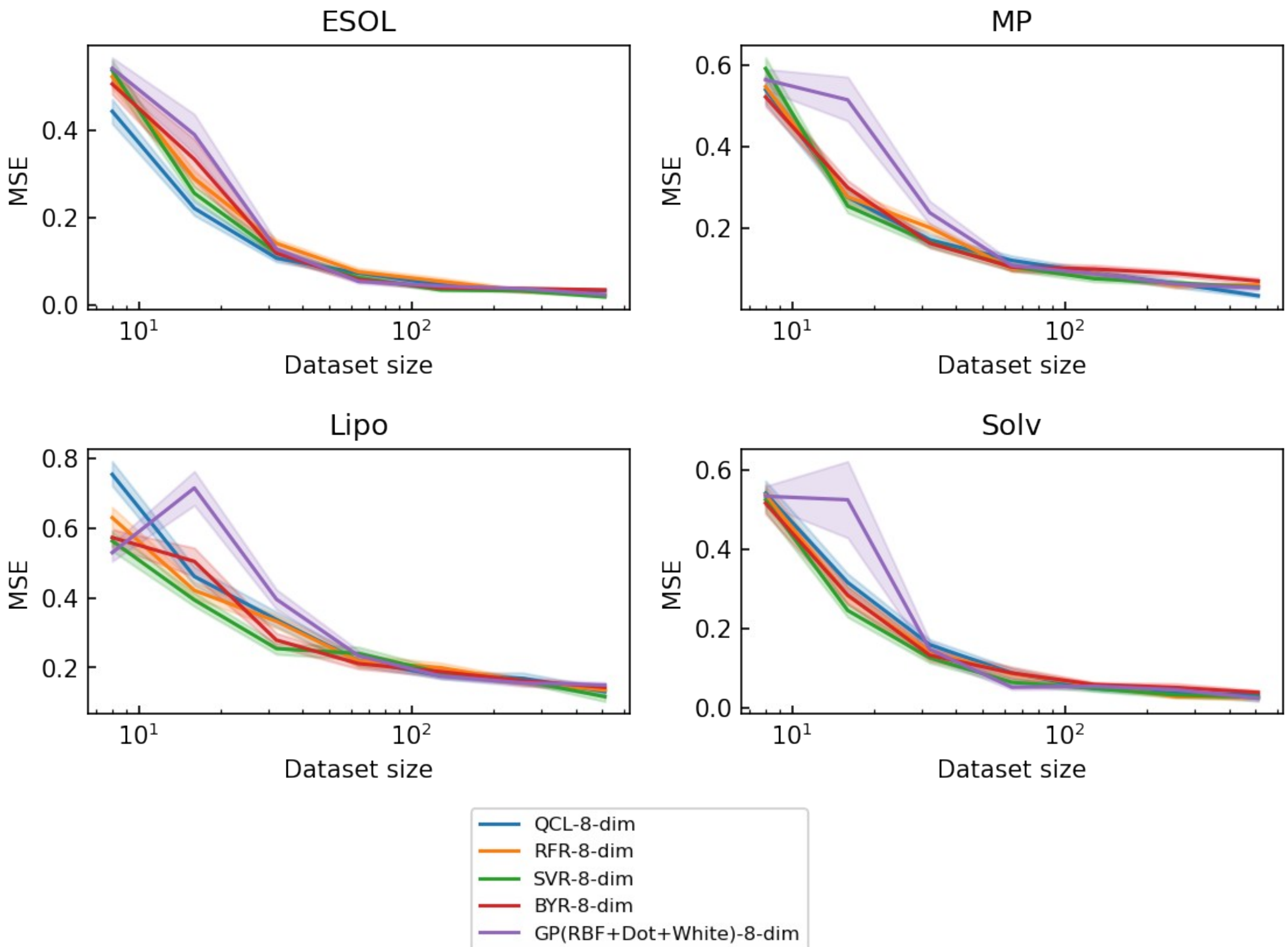

b)

Figure S 15 Regression results for the interpolating tasks as Box plots. b) Line plots with standard errors with 68% confidence intervals. In the figures, 20% of testing data were randomly sampled from the dataset, whereas the top 20% records of y were extracted in Figure S 14.

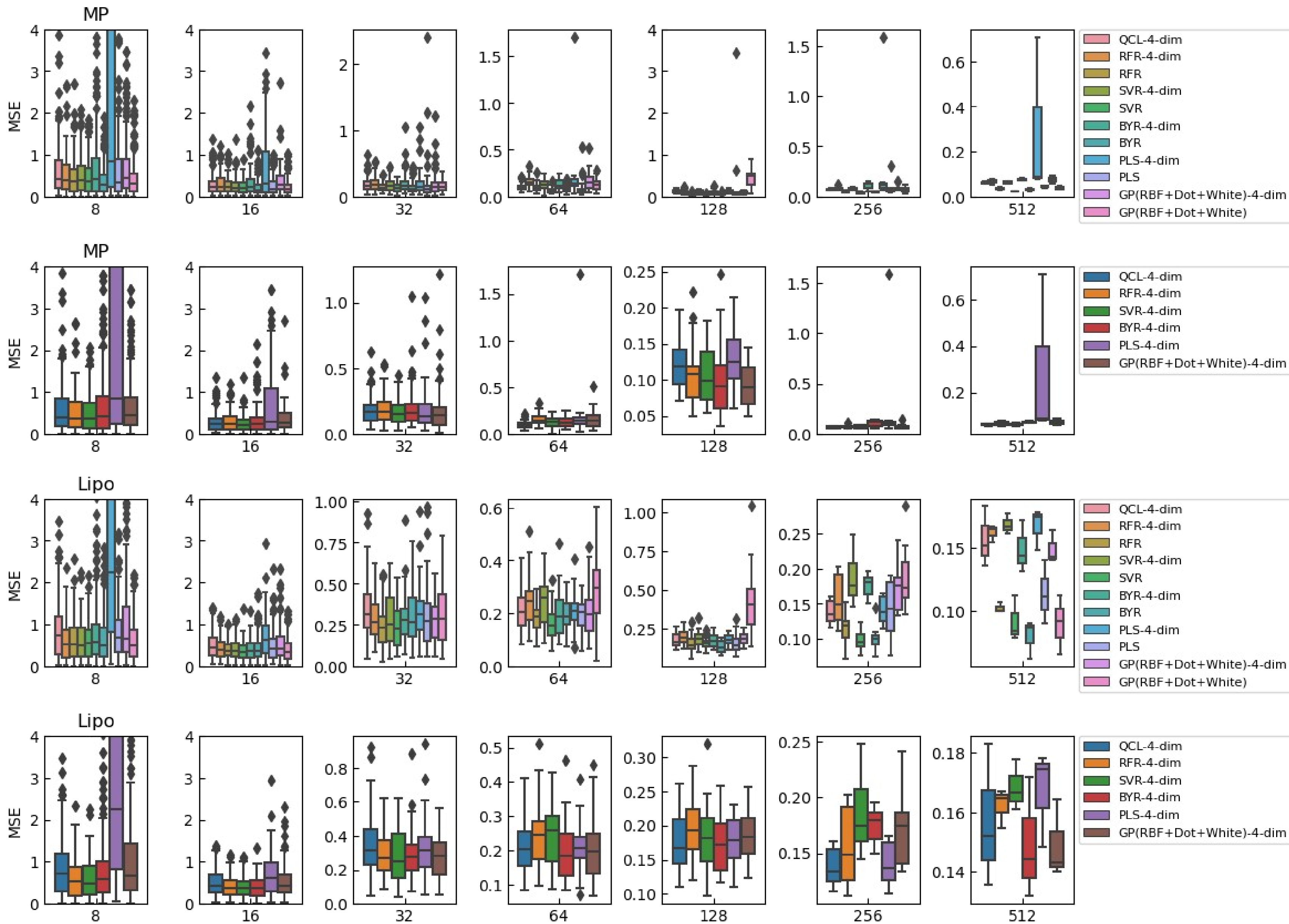
MP
MP
Lipo
Lipo
MSE
8
16
32
64
128
256
512
QCL-4-dim
RFR-4-dim
RFR
SVR-4-dim
SVR
BYR-4-dim
BYR
PLS-4-dim
PLS
GP(RBF+Dot+White)-4-dim
GP(RBF+Dot+White)

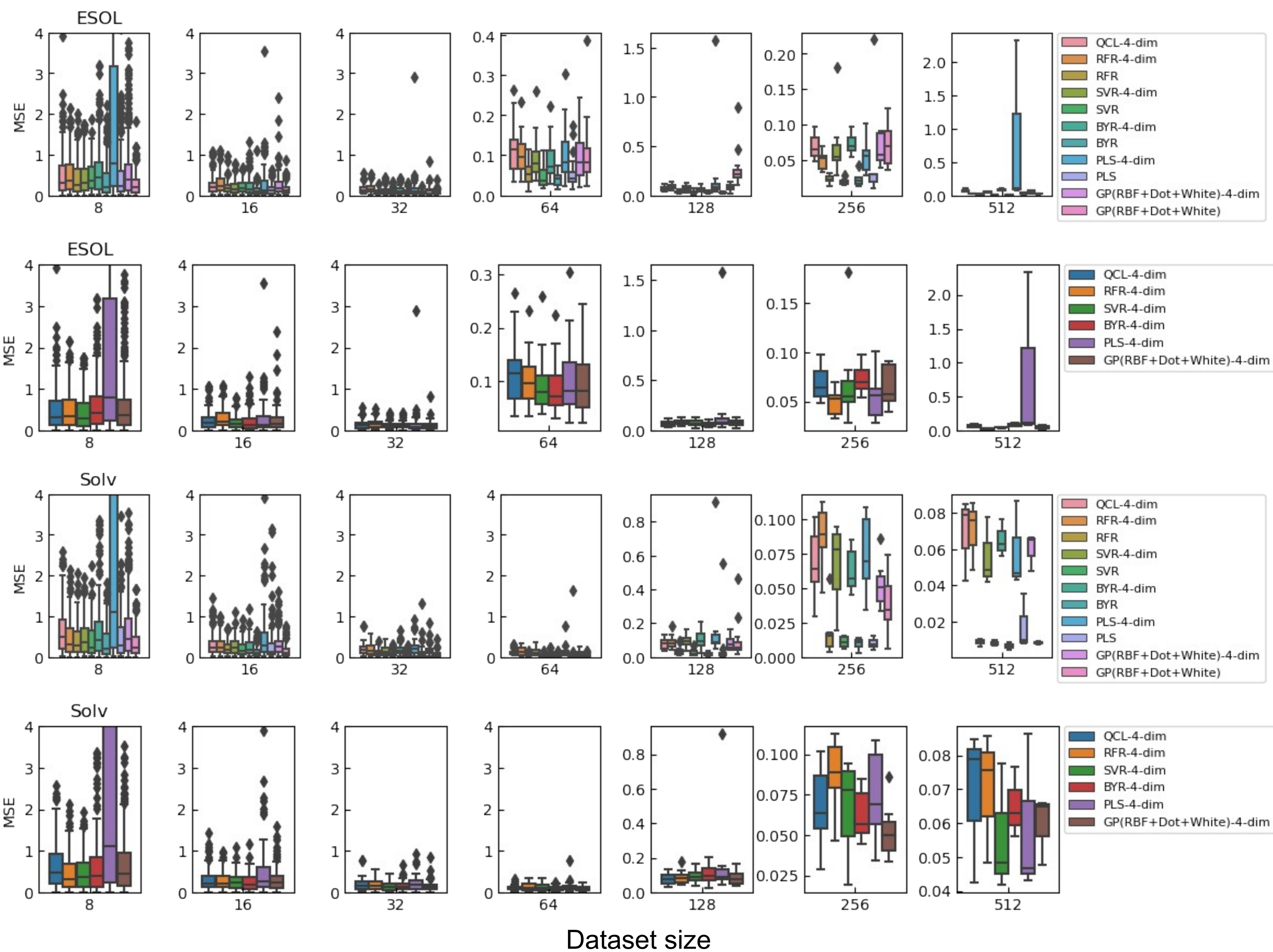
ESOL
Solv
MSE
Dataset size
QCL-4-dim
RFR-4-dim
RFR
SVR-4-dim
SVR
BYR-4-dim
BYR
PLS-4-dim
PLS
GP(RBF+Dot+White)-4-dim
GP(RBF+Dot+White)
8
16
32
64
128
256
512

a)

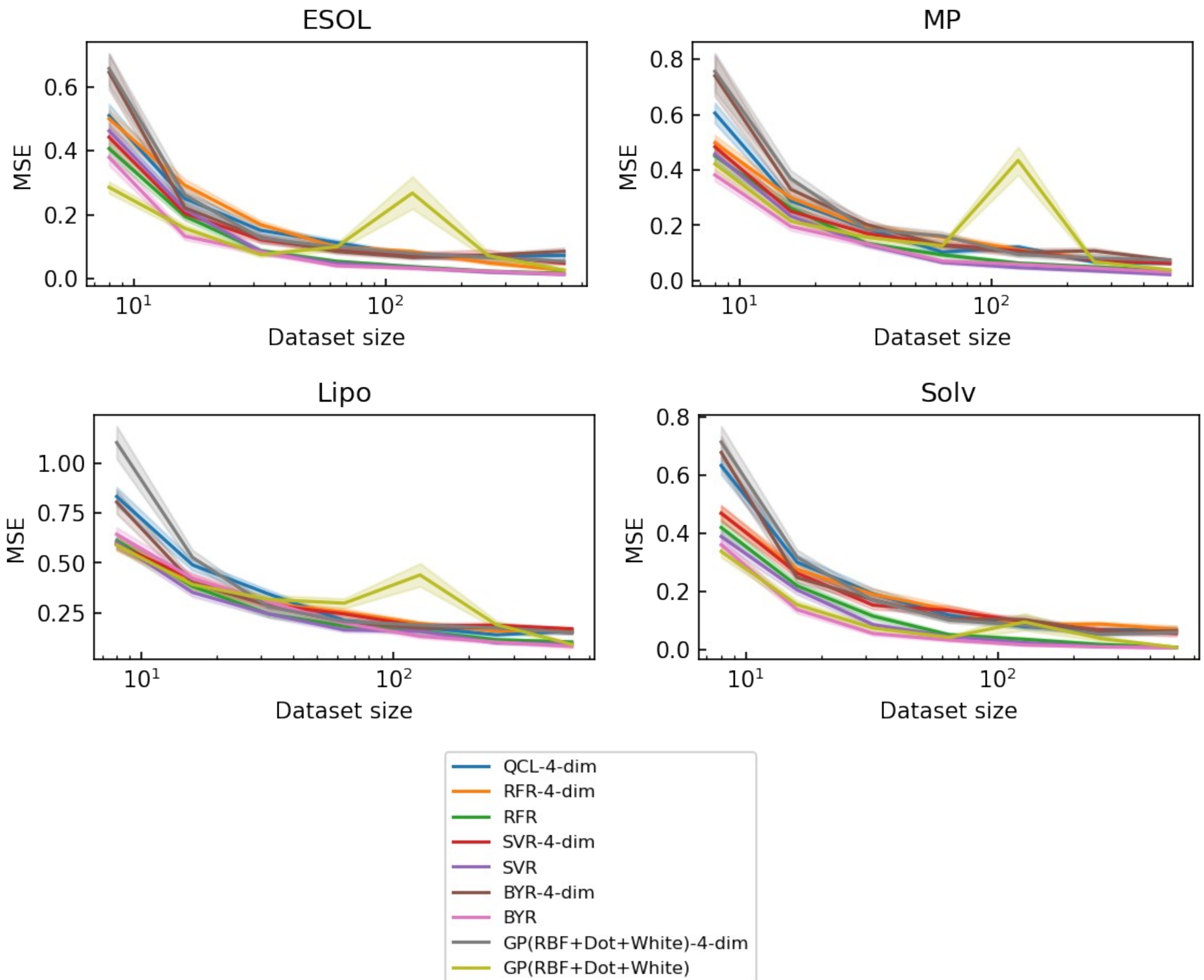

ESOL
MP
Lipo
Solv
MSE
Dataset size
QCL-4-dim
RFR-4-dim
RFR
SVR-4-dim
SVR
BYR-4-dim
BYR
GP(RBF+Dot+White)-4-dim
GP(RBF+Dot+White)

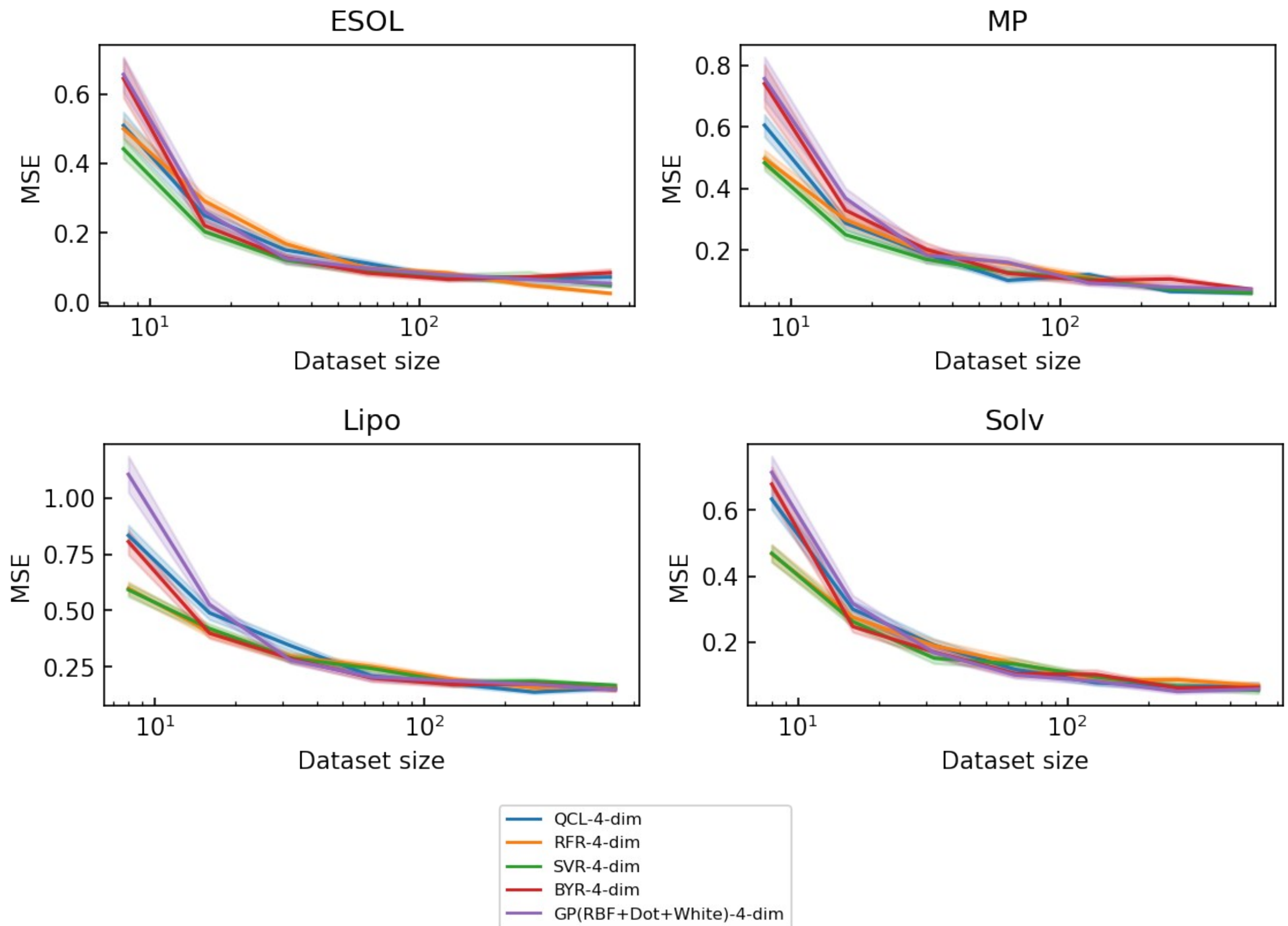

b)

Figure S 16 Regression results for the interpolating tasks with 4-dimensional vectors. a) Box plots and b) Line plots with standard errors with 68% confidence intervals.. A QCL circuit ($n = 8$) inputted a vector of $(x_1, x_1, x_2, x_2, \dots, x_4, x_4)$.

Table S4 List of molecular descriptors calculated by RDKit.

Name			
MaxEStateIndex	PEOE_VSA2	VSA_EState9	fr_aryl_methyl
MinEStateIndex	PEOE_VSA3	FractionCSP3	fr_azide
MaxAbsEStateIndex	PEOE_VSA4	HeavyAtomCount	fr_azo
MinAbsEStateIndex	PEOE_VSA5	NHOHCount	fr_barbitur
qed	PEOE_VSA6	NOCount	fr_benzene
MolWt	PEOE_VSA7	NumAliphaticCarbocycles	fr_benzodiazepine
HeavyAtomMolWt	PEOE_VSA8	NumAliphaticHeterocycles	fr_bicyclic
ExactMolWt	PEOE_VSA9	NumAliphaticRings	fr_diazo
NumValenceElectrons	SMR_VSA1	NumAromaticCarbocycles	fr_dihydropyridine
NumRadicalElectrons	SMR_VSA10	NumAromaticHeterocycles	fr_epoxide
MaxPartialCharge	SMR_VSA2	NumAromaticRings	fr_ester
MinPartialCharge	SMR_VSA3	NumHAcceptors	fr_ether
MaxAbsPartialCharge	SMR_VSA4	NumHDonors	fr_furan
MinAbsPartialCharge	SMR_VSA5	NumHeteroatoms	fr_guanido
FpDensityMorgan1	SMR_VSA6	NumRotatableBonds	fr_halogen
FpDensityMorgan2	SMR_VSA7	NumSaturatedCarbocycles	fr_hdrzine
FpDensityMorgan3	SMR_VSA8	NumSaturatedHeterocycles	fr_hdrzone
BCUT2D_MWHI	SMR_VSA9	NumSaturatedRings	fr_imidazole
BCUT2D_MWLOW	SlogP_VSA1	RingCount	fr_imide
BCUT2D_CHGHI	SlogP_VSA10	MolLogP	fr_isocyan
BCUT2D_CHGLO	SlogP_VSA11	MolMR	fr_isothiocyan
BCUT2D_LOGPHI	SlogP_VSA12	fr_Al_COO	fr_ketone

BCUT2D_LOGPLOW	SlogP_VSA2	fr_Al_OH	fr_ketone_Topliss
BCUT2D_MRHI	SlogP_VSA3	fr_Al_OH_noTert	fr_lactam
BCUT2D_MRLOW	SlogP_VSA4	fr_ArN	fr_lactone
BalabanJ	SlogP_VSA5	fr_Ar_COO	fr_methoxy
BertzCT	SlogP_VSA6	fr_Ar_N	fr_morpholine
Chi0	SlogP_VSA7	fr_Ar_NH	fr_nitrile
Chi0n	SlogP_VSA8	fr_Ar_OH	fr_nitro
Chi0v	SlogP_VSA9	fr_COO	fr_nitro_arom
Chi1	TPSA	fr_COO2	fr_nitro_arom_nonortho
Chi1n	EState_VSA1	fr_C_O	fr_nitroso
Chi1v	EState_VSA10	fr_C_O_noCOO	fr_oxazole
Chi2n	EState_VSA11	fr_C_S	fr_oxime
Chi2v	EState_VSA2	fr_HOCCN	fr_para_hydroxylation
Chi3n	EState_VSA3	fr_Imine	fr_phenol
Chi3v	EState_VSA4	fr_NH0	fr_phenol_noOrthoHbond
Chi4n	EState_VSA5	fr_NH1	fr_phos_acid
Chi4v	EState_VSA6	fr_NH2	fr_phos_ester
HallKierAlpha	EState_VSA7	fr_N_O	fr_piperdine
Ipc	EState_VSA8	fr_Ndealkylation1	fr_piperzine
Kappa1	EState_VSA9	fr_Ndealkylation2	fr_priamide
Kappa2	VSA_EState1	fr_Nhpyrrole	fr_prisulfonamd
Kappa3	VSA_EState10	fr_SH	fr_pyridine
LabuteASA	VSA_EState2	fr_aldehyde	fr_quatN
PEOE_VSA1	VSA_EState3	fr_alkyl_carbamate	fr_sulfide

PEOE_VSA10	VSA_EState4	fr_alkyl_halide	fr_sulfonamd
PEOE_VSA11	VSA_EState5	fr_allylic_oxid	fr_sulfone
PEOE_VSA12	VSA_EState6	fr_amide	fr_term_acetylene
PEOE_VSA13	VSA_EState7	fr_amidine	fr_tetrazole
PEOE_VSA14	VSA_EState8	fr_aniline	fr_thiazole
			fr_thiocyan
			fr_thiophene
			fr_unbrch_alkane
			fr_urea